Loss of C2orf69 defines a fatal autoinflammatory syndrome in humans and zebrafish that evokes a glycogen-storage-associated mitochondriopathy

Hui Hui Wong,[1] Sze Hwee Seet,[1] Michael Maier,[2] Ayse Gurel,[3] Ricardo Moreno Traspas,[2] Cheryl Lee,[1,4] Shan Zhang,[3] Beril Talim,[5] Abigail Y.T. Loh,[1] Crystal Y. Chia,[2] Tze Shin Teoh,[2] Danielle Sng,[2] Jarred Rensvold,[6,7] Sule Unal,[8,9] Evgenia Shishkova,[10,11] Ece Cepni,[12] Fatima M. Nathan,[13] Fernanda L. Sirota,[14] Chao Liang,[3] Nese Yarali,[15] Pelin O. Simsek-Kiper,[16] Tadahiro Mitani,[17] Serdar Ceylaner,[18] Ozlem Arman-Bilir,[15] Hamdi Mbarek,[19] Fatma Gumruk,[8,9] Stephanie Efthymiou,[20] Deniz Uğurlu Çïmen,[21] Danai Georgiadou,[2] Kortessa Sotiropoulou,[1] Henry Houlden,[22] Franziska Paul,[1] Davut Pehlivan,[17,23,24] Candice Lainé,[25,26] Guoliang Chai,[27,28] Nur Ain Ali,[2] Siew Chin Choo,[2] Soh Sok Keng,[1] Bertrand Boisson,[25,26,29] Elanur Yılmaz,[21] Shifeng Xue,[1,30] Joshua J. Coon,[7,10,11,31] Thanh Thao Nguyen Ly,[1,30] Naser Gilani,[32] Dana Hasbini,[33] Hulya Kayserili,[21] Maha S. Zaki,[34] Robert J. Isfort,[35] Natalia Ordonez,[36] Kornelia Tripolszki,[36] Peter Bauer,[36] Nima Rezaei,[37,38] Simin Seyedpour,[40] Ghamar Taj Khotaei,[39] Charles C. Bascom,[35] Reza Maroofian,[20] Myriam Chaabouni,[40] Afaf Alsubhi,[41,42] Wafaa Eyaid,[41,42] Sedat Işıkay,[43] Joseph G. Gleeson,[27,28] James R. Lupski,[17,23,24,44] Jean-Laurent Casanova,[25,26,29,45,46] David J. Pagliarini,[6,7,10,47,48,49] Nurten A. Akarsu,[3] Sebastian Maurer-Stroh,[14] Arda Cetinkaya,[3] Aida Bertoli-Avella,[36] Ajay S. Mathuru,[1,13,50] Lena Ho,[1,4,52] Frederic A. Bard,[1,52,53,*] and Bruno Reversade[1,2,21,51,52,53,*]

Summary

Human *C2orf69* is an evolutionarily conserved gene whose function is unknown. Here, we report eight unrelated families from which 20 children presented with a fatal syndrome consisting of severe autoinflammation and progredient leukoencephalopathy with recurrent seizures; 12 of these subjects, whose DNA was available, segregated homozygous loss-of-function *C2orf69* variants. C2ORF69 bears homology to esterase enzymes, and orthologs can be found in most eukaryotic genomes, including that of unicellular phytoplankton. We found that endogenous C2ORF69 (1) is loosely bound to mitochondria, (2) affects mitochondrial membrane potential and oxidative respiration in cultured neurons, and (3) controls the levels of the glycogen branching enzyme 1 (GBE1) consistent with a glycogen-storage-associated mitochondriopathy. We show that CRISPR-Cas9-mediated inactivation of zebrafish *C2orf69* results in lethality by 8 months of age due to spontaneous epileptic seizures, which is preceded by persistent brain inflammation. Collectively, our results delineate an autoinflammatory Mendelian disorder of *C2orf69* deficiency that disrupts the development/homeostasis of the immune and central nervous systems.

[1]Institute of Molecular and Cell Biology, A*STAR, Biopolis, Singapore 138673, Singapore; [2]Laboratory of Human Genetics & Therapeutics, Genome Institute of Singapore, A*STAR, Biopolis, Singapore 138672, Singapore; [3]Department of Medical Genetics, Faculty of Medicine, Hacettepe University, Ankara 06230, Turkey; [4]Cardiovascular and Metabolic Diseases, Duke-NUS Medical School, Singapore 169857, Singapore; [5]Pediatric Pathology Unit, Department of Pediatrics, Faculty of Medicine, Hacettepe University, Ankara 06230, Turkey; [6]Department of Cell Biology and Physiology, Washington University School of Medicine, St. Louis, MO 63110, USA; [7]Morgridge Institute for Research, Madison, WI 53715, USA; [8]Pediatric Hematology Unit, Department of Pediatrics, Faculty of Medicine, Hacettepe University, Ankara 06230, Turkey; [9]Research Center of Fanconi Anemia and Other Inherited Bone Marrow Failure Syndromes, Hacettepe University, Ankara 06230, Turkey; [10]National Center for Quantitative Biology of Complex Systems, Madison, WI 53562, USA; [11]Department of Biomolecular Chemistry, University of Wisconsin–Madison, Madison, WI 53562, USA; [12]Institute of Health Sciences, Koç University, 34010 Istanbul, Turkey; [13]Yale-NUS College, 12 College Avenue West, Singapore 138610, Singapore; [14]Bioinformatics Institute, A*STAR, Biopolis, Singapore 138671, Singapore; [15]Ankara Child Health and Diseases Hematology Oncology Training and Research Hospital, Ankara 06110, Turkey; [16]Pediatric Genetics Unit, Department of Pediatrics, Faculty of Medicine, Hacettepe University, Ankara 06230, Turkey; [17]Department of Molecular and Human Genetics, Baylor College of Medicine, Houston, TX 77030, USA; [18]Intergen Genetic Diagnosis Center, Ankara 06680, Turkey; [19]Qatar Genome Program, Qatar Foundation Research, Development and Innovation, Qatar Foundation, Doha, Qatar; [20]Molecular and Clinical Sciences Institute, St. George's University of London, Cranmer Terrace, London SW17 0RE, UK; [21]Medical Genetics Department, Koç University School of Medicine, 34010 Istanbul, Turkey; [22]Department of Neuromuscular Diseases, UCL Queen Square Institute of Neurology, Queen Square, London WC1N 3BG, UK; [23]Department of Pediatrics, Baylor College of Medicine, Houston, TX 77030, USA; [24]Texas Children's Hospital, Houston, TX 77030, USA; [25]Paris University, Imagine Institute, Paris 75015, France; [26]Laboratory of Human Genetics of Infectious Disease, Necker Branch, INSERM U1163, Paris, France; [27]Rady Children's Institute for Genomic Medicine, San Diego, CA 92123, USA; [28]Department of Neurosciences, University of California, San Diego, La Jolla, CA 92093, USA; [29]St. Giles Laboratory of Human Genetics of Infectious Diseases, Rockefeller Branch, The Rockefeller University, New York, NY 10065, USA; [30]Department of Biological Sciences, National University of Singapore, Singapore 117558, Singapore; [31]Department of Chemistry, University of Wisconsin–Madison, Madison, WI 53562, USA; [32]Farabi Medical Laboratory, Erbil, Iraq; [33]Chief Division Pediatric Neurology, Department of Pediatrics, Rafic Hariri University Hospital, Beirut, Lebanon; [34]Clinical Genetics Department, National Research Centre, Cairo 12622, Egypt; [35]Corporate Research, The Procter and Gamble Company, Cincinnati, OH 45040, USA; [36]Genomic Research, CENTOGENE GmbH, 18055 Rostock, Germany; [37]Research Center for Immunodeficiencies, Children's Medical Center, Tehran

(Affiliations continued on next page)

Introduction

The mitochondrial proteome is composed of about ~1,100 proteins, and fewer than a thousand are shared with yeast.[1] With the exception of 13 proteins encoded by the mitochondrial genome (mtDNA), all other proteins of the mitochondrial proteome are encoded by the nuclear genome. As such, the vast majority of human diseases with mitochondrial defects, or mitochondriopathies, result from mutations in the nuclear rather than the mtDNA genome.[2] In addition to their canonical role of ATP generation through oxidative phosphorylation (OXPHOS), mitochondria play a host of varied functions, ranging from regulation of apoptosis and metabolism of amino acids and lipids to calcium handling and reactive oxygen species (ROS) regulation. Primary mitochondrial disorders, such as Leigh syndrome (MIM: 256000), are often caused by pathogenic variants in mitochondrial proteins that result in bioenergetic defects.[3] Other inherited mitochondrial defects arise from impairments in lipid metabolism,[4] control of cell death,[5] organellar and protein quality control,[6] fission and fusion, metabolite biogenesis[7] that impacts OXPHOS, and other cellular processes dependent on mitochondrial integrity. Despite extensive efforts to catalog the mitochondrial proteome,[8] many proteins remain uncharacterized.

While mitochondrial disorders are clinically heterogeneous and can affect any organ system with varying degrees of severity and age of onset,[9] mitochondriopathies often present as central nervous system diseases, consistent with their intense energy demand and high mitochondria content. Similarly, there is a preponderance of common neurological disorders with a mitochondrial basis.[10] Even within the brain, systemic proteomic analysis has revealed differences in mitochondrial composition across neuronal subtypes,[11] reflecting exquisite functional specificity. Brain mitochondria are required for axonal differentiation, synaptic branching, synaptic transmission, and metabolite production.[12] In addition, mitochondria are intimately involved in regulating innate immunity in the brain.[13] For these reasons, many mitochondriopathies are characterized by epilepsy,[14] microcephaly, and neuroinflammation.[15]

Here, we identify and report on the clinical, genetic, and cellular characterization of a mitochondriopathy with autoinflammatory aspects that is driven by bi-allelic pathogenic variation in *C2orf69* (MIM: 619219), a protein-coding gene with no known function.

Methods

Human study participants

All procedures followed were in accordance with the ethical standards of the responsible committee on human experimentation (institutional and national) and proper informed consent was obtained. We withdrew peripheral blood samples from all available family members to extract genomic DNA (gDNA) by using DNeasy Blood and Tissue Kits (QIAGEN). All bio-specimens were obtained after written informed consents were signed from participants or their legal guardians. All human studies were reviewed and approved by the Rockefeller University Hospital (New York, US), Hacettepe University Ethics Committee (GO15/721, GO19/604), or the institutional review boards of A* STAR (2019-087).

Exome and Sanger sequencing

Parents and their children were genotyped with Illumina Humancore-12v1 BeadChips following the manufacturer's instructions. Call rates were above 99%. Gender and relationships were verified with Illumina BeadStudio. Exome sequencing was performed on gDNA from libraries prepared on an Ion One-Touch System and sequenced on an Ion Proton instrument (Life Technologies). Sequence reads were aligned to the human GRCh37/hg19 assembly (UCSC Genome browser). Each variant was annotated with the associated gene, location, protein position, amino acid change, quality score, and coverage. Variants were filtered for common SNPs with the NCBI's "common and no known medical impacts" database, the Genome Aggregation Consortium, and the Exome Sequencing Project as well as in-house databases of sequenced individuals, mainly of Middle East origin. Homozygous variants were further filtered on the basis of functional prediction scores, including SIFT, PolyPhen-2, and M-CAP.[16]

CRISPR-Cas9 editing

Zebrafish were maintained and used according to the Singapore National Advisory Committee on Laboratory Animal Research Guidelines. Two guide RNAs against exon 1 of *c2orf69* were used

University of Medical Sciences, Tehran 14194, Iran; [38]Network of Immunity in Infection, Malignancy and Autoimmunity, Universal Scientific Education and Research Network, Tehran 14197, Iran; [39]Department of Pediatric Infectious Diseases, Children's Medical Center, Tehran University of Medical Sciences, Tehran 14194, Iran; [40]Laboratoire d'analyses spécialisé en Génétique, Tunis 1082, Tunisia; [41]Division of Genetics, Department of Pediatrics, King Abdullah Specialized Children Hospital, King Abdulaziz Medical City, MNGHA, Riyadh 14611, Saudi Arabia; [42]King Abdullah International Medical Research Center, King Saud bin Abdulaziz University for Health Sciences, MNGHA, Riyadh 11481, Saudi Arabia; [43]Department of Pediatrics, Division of Neurology, University of Gaziantep, School of Medicine, Gaziantep 27310, Turkey; [44]Human Genome Sequencing Center, Baylor College of Medicine, Houston, TX 77030, USA; [45]Pediatric Immunology-Hematology Unit, Assistance Publique-Hôpitaux de Paris, Necker Hospital for Sick Children, Paris 75015, France; [46]Howard Hughes Medical Institute, New York, NY 10065, USA; [47]Department of Biochemistry and Molecular Biophysics, Washington University School of Medicine, St. Louis, MO 63110, USA; [48]Department of Genetics, Washington University School of Medicine, St. Louis, MO 63110, USA; [49]Department of Biochemistry, University of Wisconsin–Madison, Madison, WI 53706, USA; [50]Department of Physiology, Yong Loo Lin School of Medicine, National University of Singapore, Singapore 117593, Singapore; [51]Department of Paediatrics, Yong Loo Lin School of Medicine, National University of Singapore, Singapore 119228, Singapore
[52]These authors contributed equally
[53]Senior author
*Correspondence: fbard@imcb.a-star.edu.sg (F.A.B.), bruno@reversade.com (B.R.)
https://doi.org/10.1016/j.ajhg.2021.05.003.

with the following targeting sequences: 5′-AGAGCAGAACAT CATTGACG-3′ and 5′-GGAAAATGACCGCTGCAACG-3′. gRNAs were synthesized with a MEGAshortscript Kit (Thermo Fisher) according to the manufacturer's protocol and purified with an RNeasy Mini Kit (QIAGEN). 1 nL of a mixture containing 500 ng/μL gRNA and 0.1 mg/mL Cas9 protein was injected into the yolk of 1-cell AB zebrafish embryos. We selected, raised, and outbred two independent lines to eliminate potential off-target mutations.

Pentylenetetrazole-treated convulsion test assay

Zebrafish behavioral experiments were conducted according to approved protocol (A*STAR IACUC #: 191501). As described previously,[17] videos of larval zebrafish at 50 fps (frames per second) were acquired and analyzed for locomotion changes in response to pentylenetetrazole (PTZ) 5 mM (final concentration in the well; Pentylenetetrazole Sigma, CAS Number 54-95-5) treatment. Briefly, 2-min videos of 7–11 days post fertilization (dpf) larvae in 24-well flat bottom plates were acquired on custom designed hardware via a Basler Ace (acA1300-200um; 1,280 × 1,024) camera with a 25 mm lens attachment placed 65 cm above the plate. The 24-well plate was prefilled with 1 mL 2% agarose and backlit by a uniform white light LED lightbox. Larvae were gently delivered singly into each well via a dropper and acclimated for 5 min. Five videos of 2 min each were acquired. PTZ or system water (control) was pipetted into each well after the first video. Larvae were tracked online during video recording on a custom written software in LabView. Low-, medium-, and high-speed swim bouts were defined as 0 to 8 mm/sec, 8 to 16 mm/sec, and >16 mm/sec, respectively, as suggested.[18] Tracks, distance traveled, velocity, and immobility frequency were calculated automatically with custom written scripts in Python.

Adult fish study was performed in a similar manner. Briefly, fish were netted from the home tank in pairs and transferred to the behavior examination room. They were then transferred into two observation chambers with 150 mL of 5 mM PTZ placed against a black background and were uniformly illuminated by a white light LED lightbox. A Basler Ace (acA1300-200um; 1,280 × 1,024) camera placed in front of the tanks at ~40 cm distance recorded videos at 50 fps for 15 min. Latency to tonic and clonic seizure-like behavior was scored according to the protocol chapter[19] described for adult responses to PTZ treatment.

Quantitative real time PCR

Total RNA was isolated from fibroblast cultures with an RNeasy kit (QIAGEN, #74106) according to the manufacturer's protocol. 1 μg of RNA was reverse transcribed with the Superscript III First-Strand Synthesis System (Invitrogen, #18080-051). Products were amplified with SYBR Green PCR Master Mix (Applied Biosystems, #4309155) on an Applied Biosystems 7500 Real-Time PCR System. We performed each reaction in triplicate and averaged and normalized data to mean β-actin RNA levels to obtain the respective ΔCT (cycle threshold) value.

Seahorse analysis

10,000 BJ-TERT fibroblast cells were plated on Seahorse XF96 Cell Culture Microplates (Agilent). For MitoStress assay, 2 μM of oligomycin (Sigma), 1 μM of FCCP (Carbonyl cyanide 4-(trifluoromethoxy) phenylhydrazone) (Sigma), and 1 μM of Rotenone/Antimycin (Sigma/Sigma) were injected according to Seahorse MitoStress assay protocol (Agilent). MitoStress test data were obtained via XF96 Seahorse Wave software (Agilent). We performed citrate synthase normalization assay on the cultured cell plate to normalize the measured oxygen consumption rate (OCR) and extracellular acidification rate (ECAR). 2,000 ReNcell VM neurons were plated on Seahorse XF96 Cell Culture Microplates and differentiated for 14 days prior to siRNA-mediated knockdown of C2orf69. Cells were subjected to MitoStress assay 3 days post transfection as described above.

Cell lines, cell culture media, and reagents

The parental BJ-TERT fibroblasts, human newborn foreskin fibroblasts immortalized with the telomerase reverse transcriptase, were provided by Procter and Gamble (Cincinnati, USA). The cell line is maintained in Fibroblast Basal Medium (#PCS-201-030) and was supplemented with Fibroblast Growth Kit-Low serum (#PCS-201-041) with a final concentration of 5 ng/mL recombinant human fibroblast growth factor (FGF) basic, 7.5 mM L-glutamine, 50 μg/mL ascorbic acid, 1 μg/mL hydrocortisone hemisuccinate, 5 μg/mL recombinant human insulin, and 2% fetal bovine serum, purchased from the American Type Culture Collection (ATCC, Manassas, VA). HEK293T cells were maintained with DMEM containing 10% fetal bovine serum (FBS). ReNcell VM human neural progenitor cell lines (Sigma Aldrich) were maintained in ReNcell NSC Maintenance medium (Sigma Aldrich) supplemented with 20 ng/mL of epidermal growth factor (EGF) (Thermo Fisher) and basic fibroblast growth factor (bFGF) (Thermo Fisher). Cells were differentiated in the same medium, but EGF and bFGF were replaced with 10 ng/mL of glial cell line-derived neurotrophic factor (GDNF) (Thermo Fisher) and brain-derived neurotrophic factor (BDNF) (Thermo Fisher) for 2 weeks with a change of media every 3 days. Cells were seeded on culture flasks or plates pre-coated overnight at 4°C with 20 μg/mL laminin (Thermo Fisher) in DPBS. The cells were subcultured approximately every 5 days at 90% confluence by detaching them with Accutase (Millipore). All cells were grown at 37°C in a 5% CO_2 incubator. MG132 was purchased from Sigma Aldrich. Cells were treated with 20 nM of MG132 for 20 h prior to lysis for immunoblot analysis.

The haploid HAP1 wild-type (WT) and knockout (KO) cells (Horizon Discovery: WT, C631; C2orf69 KO1, HZGHC005743c010; C2orf69 KO2, HZGHC005744c004; GBE1 KO, HZGHC006051c010) were cultured in Iscove's Modified Dulbecco's Media (Thermo Fisher, 12440053) with 10% FBS (Sigma, F2442) and 1× penicillin-streptomycin (Thermo Fisher, 15140122) at 37°C and 5% CO_2.

Immunoblotting

We prepared protein lysates from cultured cells by scraping in lysis buffer composed of 150 mM NaCl, 1% IGEPAL CA-630, 0.5% sodium deoxycholate, 0.1% SDS, 50 mM Tris (pH 8.0), 0.4 mM EDTA (pH 8.0), 10% glycerol, and protease inhibitors (Sigma, 11836170001) while on ice and transferred them into microcentrifuge tubes. The extracts were clarified by centrifugation (16,000 g, 15 min, 4°C), and the supernatants were transferred to new tubes. Then 20 μg of cleared whole-cell lysate, as determined by BCA assay (Thermo Fisher, 23225), was separated on a NuPAGE 4%–12% Bis-Tris gel (Thermo Fisher, NP0323BOX) with a protein standard (Thermo Fisher, LC5800), transferred to PVDF membrane (Sigma, IPFL00010), probed with primary antibodies (GBE1,

Proteintech, 20313-1-AP; GBE1, Abcam, ab180596; VDAC1, Abcam, ab18988; ACTB, Abcam, ab8224), and analyzed with a LI-COR Odyssey CLx Imaging System and LI-COR Image Studio Software (v.5.2.5) with secondary antibodies (LI-COR: 926-32211, 926-68070).

Muscle histopathology

Skeletal muscle biopsy was fresh frozen in isopentane at liquid nitrogen temperature and 8 μm-thick cryosections were used for routine diagnostic batch of histochemical stains, including hematoxylin-eosin, modified Gomori trichrome, periodic acid-Schiff (PAS), PAS-diastase, Oil Red O, nicotinamide adenine dinucleotide tetrazolium reductase (NADH), succinate dehydrogenase (SDH), cytochrome *c*-oxidase (COX), COX-SDH (COX-succinate dehydrogenase), and adenosine triphosphatase (ATPase).[20]

Cellular fractionation and mitochondrial extraction

Cytosolic, membrane, and nuclear protein extracts were obtained via the Cell Fractionation Kit Standard (Abcam #ab109719) according to the manufacturer's instructions. Proteinase K protection and extraction assays on isolated mitochondria were performed as previously described.[21] We gently resuspended mitochondria pellet in the isotonic buffer to get protein concentration at 1 mg/mL. For extraction assays, aliquots of mitochondria were solubilized by increasing concentrations of digitonin (0% to 0.22%) for 1 h at 4 °C. Soluble and insoluble fractions were separated by centrifugation at 20,000 × *g* for 20 min. Insoluble fractions were fully resuspended in an equal amount of isotonic buffer to match the volume of supernatant. Both fractions were lysed in 1× Laemmli sample buffer and analyzed by SDS-PAGE and immunoblotting. For proteinase K (PK) protection assays, we then added PK to 100 μg/mL and incubated it for 30 min on ice to allow the complete digestion of accessible proteins. To terminate the protease digestion, we freshly prepared PMSF and added it to a concentration of 8 mM. Samples were analyzed by western.

Protein quantification was performed with the PierceTM BCA Protein Assay Kit (Thermo Fisher #23225). For immunoblotting, samples were reduced in Laemmli loading buffer containing dithiothreitol and denatured at 95°C for 5 min. Protein samples were loaded into 4%–20% Criterion TGX Precast Midi Protein Gels (Bio-Rad #5671093) in 1× running buffer (25 mM Tris, 200 mM Glycine, 0.1% sodium dodecyl sulfate) and electrophoresed at 120 V until desired separation. Proteins were transferred from the polyacrylamide gel onto a 0.2 μm Immun-Blot Low Fluorescence PVDF Membrane (Bio-Rad #1620261) via the Trans-Blot Turbo Transfer System (Bio-Rad) for 7 min. Membranes were blocked for 1 h at room temperature with 5% milk or 5% BSA in Tris-buffered saline, Tween and then incubated with the primary antibody overnight at 4°C. Antibodies used are listed in the supplemental information.

Respiratory enzymatic assays (RCAs)

We isolated zebrafish muscle homogenates from adult zebrafish skeletal muscle and brain by disrupting dissected tissues in mitochondria isolation buffer (67 mM sucrose, 50 mM KCl, 1 mM EDTA, 0.2% fatty acid free BSA, 50 mM Tri-HCl, pH 7.4) with a Dounce homogenizer tight pestle operated at 1,300 rpm. Homogenate were subjected to RCA according to Spinazzi et al.[22] with the following input quantities: 8 μg for CI, 4 μg for CII, 1.5 μg for CIII, and 1 μg for CIV. We normalized all kinetic activity measurements with citrate synthase enzyme activity of the same sample to account for differences in mitochondrial content.

Transfection by electroporation

Electroporation of C2ORF69 constructs was performed with the Neon Transfection System (Invitrogen). Briefly, cells were trypsinized, pelleted, washed, and resuspended in Resuspension Buffer R at cell density of 7×10^5 cells. The cell suspensions were mixed with 30 μg of plasmid in sterile 1.5 mL microcentrifuge tube brought to a final volume of 120 μL cell suspension with Buffer R. Electroporation was then carried out at two pulses at 1,400 V and 10 ms according to the manufacturer's instructions.

MitoTracker Red CMXRos and immunofluorescence

Transfected and control cells on coverslips were incubated with 200 nM of MitoTracker Red CMXRos (Invitrogen) for 15 min at 37°C prior to fixation with 4% paraformaldehyde in PBS. Cells were permeabilized with 0.2% Triton-X and incubated with a monoclonal mouse antibody raised against FLAG (Sigma Aldrich) at a 1:250 dilution. Mouse anti-FLAG staining was detected with an Alexa488 conjugated Donkey anti-mouse secondary antibody (Molecular Probes). Stained cells were mounted in FluoSave Mounting Medium (Millipore). Images were acquired with 40× oil immersion objective on a Zeiss LSM700 confocal microscope. Image analysis was performed with Fiji software.[23]

siRNA transfection

BJ-TERT fibroblasts were reverse transfected with final concentration of 25 nM of non-targeting control siRNA (#D-001210-03-50, Dharmacon) or C2ORF69 siRNA (#M-018633-01-0005, Dharmacon) complexed with Lipofectamine RNAiMAX (Invitrogen) in Opti-MEM (Invitrogen) according to operating instructions. The siRNA and transfection reagent were mixed for 20 min prior to transfection. siRNA silencing in differentiated ReNcell VM (10 days) was performed with similar preparation but via forward transfection with Lipofectamine RNAiMAX Reagent in 96-well format.

Blue and clear native PAGE

We further isolated mitochondria by centrifuging the homogenates described above at 600 × *g* for 5 min to clear intact myofibrils and heavy cell debris and then spun them at 7,000 × *g* for 15 min to isolate the desired mitochondrial fraction. 50 μg of purified mitochondria were extracted with 8 g/g digitonin and resolved on 3%–12% native PAGE gels (Thermo Fisher) for immunoblotting (blue native) or complex I in-gel assay (clear native) according to manufacturer's instructions.[24]

Mitochondrial membrane potential and ROS measurements

The concentrations used for TMRE (tetramethylrhodamine, ethyl ester) (Thermo Fisher T669), JC-1 (Life Technologies 65-0851-38), and mitoSOX (Thermo Fisher M36008) were 100 nM, 1 μM, and 5 μM, respectively. Cells were incubated in culture media (BJ fibroblasts) or HBSS (5.6 mM glucose + 1% BSA) with the dyes for 30 min at 37°C. The cells were then washed with warm PBS, trypsinized and pelleted before resuspending in warm media for acquisition by flow cytometry or imaged immediately on the Operetta system (Perkin Elmer). For JC-1 measurements, cells were imaged in both Y3 and GFP channels under non-saturating parameters. The ratio between Y3 and GFP (red/green) was obtained by segmenting on

the Y3 channel at a threshold that accurately selected all JC-1-positive mitochondria.

Results

A recessive Mendelian disorder caused by *C2orf69* deficiency

We initiated this study with the clinical investigation of two affected brothers born to consanguineous parents of Kurdish Turkish origin (Figures 1A and 1C). Both siblings presented with multisystem involvement in the first 3 months of the postnatal period (Table 1). The clinical findings were failure to thrive, global developmental delay, periodic fevers with elevated C-reactive protein, hypochromic microcytic anemia, and episodes of septic and aseptic osteomyelitis and/or arthritis. At 12 months of age, the index individual, I:2, showed progredient and severe microcephaly with a head circumference of 39 cm, exceeding −5 standard deviation (SD). Cranial MRI revealed prominent leukoencephalopathy with cerebellar atrophy/Dandy-Walker variant, corpus callosum dysgenesis, and diffuse hypomyelination (Figures 1C and 1D). Both brothers experienced recurrent seizures. Proband II:1 from family 1 (F1) died of pneumonia at 18 months of age. Exome sequencing (ES) revealed a potentially disease-causing germline homozygous frameshift variant (c.298del [p.Gln100Serfs*18] [GenBank: NM_153689.5]) in chromosome 2 open-reading frame 69 (*C2orf69*, MIM: 619219). Sanger sequencing confirmed that both neurotypical parents are heterozygous for this variant, which was found to fulfill Mendelian expectations for an autosomal recessive trait in the younger affected brother II:2 (family 1).

Eighteen other similarly affected children, nine girls and nine boys, from seven additional families originating from Tunisia (family 2 [F2]), Saudi Arabia (family 3 [F3]), Iran (family 4 [F4]), Egypt (family 5 [F5]), Syria (family 6 [F6]), Iraq (family 7 [F7]), and Turkey (family 8 [F8]) were recruited through existing collaborations (Figure 1A). All children shared a triad of symptoms consisting of brain atrophy with progressive leukoencephalopathy and recurrent seizures, septic inflammation, and failure to thrive (Table 1). Of the 20 affected children, 12 could be shown to have inherited homozygous damaging *C2orf69* variants, while eight others, who had died before this study began, were unavailable for testing (Figure 1A). In the affected individual from F8, developmental and epileptic encephalopathy is accompanied by congenital dyserythropoietic anemia (MIM: 615631). The detailed clinical features of each family can be found in the supplemental notes.

According to gnomAD (v.2.1.1 and v.3.1), no homozygous damaging variants have been reported for *C2orf69*. The three frameshift variants, c.298del (p.Gln100Serfs*18) of families 1, 4, and 7, c.280delG (p.Glu94Serfs*24) of family 2, and c.909_925del (p.Ser304Leufs*29) of family 6, and stop-gained c.929G>A (p.Trp310*) mutations of family 8 have not been reported in public databases (gnomAD, BRAVO/TOPmed) or in combined in-house databases consisting of >50,000 exomes/genomes. The c.588_592delTTTAA (p.Asn196Lysfs*4) variant from family 3 is rare and was reported seven times before in the heterozygous state (rs775817125; MAF = 2×10^{-5}). All five truncating variants were predicted to be deleterious and had combined annotation-dependent depletion (CADD) scores above 30 (Figure 1B). The in-frame deletion/insertion c.311_313del (p.Leu104_Tyr105delinsHis) variant identified in II:1 from family 5 is annotated as a possible non-damaging change by MutationTaster and has a computed CADD value of 22.4. *C2orf69* has a residual variation intolerance score (RVIS) of 0.39 (placing it in the top 76% of human genes most intolerant to genetic variation) and a pLOF observed/expected score of 0.38 (gnomAD), suggesting that *C2orf69* is a target of negative selection. Overall, these clinical and genetic findings suggest that homozygosity for pLOF variants is exceedingly rare in the general population and that the *C2orf69* variants observed in these eight kindreds are probably deleterious, most likely revealing the genetic etiology for this heretofore unknown fatal autoinflammatory and neurodevelopmental disorder (NDD).

C2orf69 is an evolutionarily conserved protein in most eukaryotic species

Genomic sequence analysis revealed that human *C2orf69* is encoded by two exons on chromosome 2q33.1 (hg19) (Figure 2A). The four identified frameshift variants are expected to significantly alter the length of the encoded protein Q8N8R5, which in humans, is predicted to be 385 amino acids long and consist of an N-terminal mitochondrial targeting signal (MTS) rich in arginine followed by a UPF0565 domain of unknown function. C2orf69 orthologs, identified with reciprocal best BLAST hits search against GenBank,[25] can be found in most eukaryotic genomes, in all metazoans, some plant genomes, and unicellular organisms, such as the phytoplankton *Emilia huxleyi* (Figure 2C). Surprisingly, no ortholog was detected in fungal genomes. Remote structure prediction and modeling with HHpred and Modeler[26] identified multiple significant hits to proteins from the hydrolase fold family, suggesting C2ORF69 may encode an enzyme belonging to the class of esterases or lipases (Figure 2D). Consistently, the hydrophobic core and predicted catalytic site are invariant for the serine 264 in all sequences analyzed (Figure 2B). The low complexity portion between residues 200 and 250 is presumably not part of the globular fold. In insect sequences, such as *Drosophila*, this central loop is significantly extended by ∼100 residues. The p.Leu104_Tyr105delinsHis variant observed in subject II:1 of family 5 is part of a highly conserved portion of residues (Figure 2B) that are at the hydrophobic core in the center of the hydrolase fold (Figure 2D) and would most likely disrupt the 3D structure of this presumed enzyme.

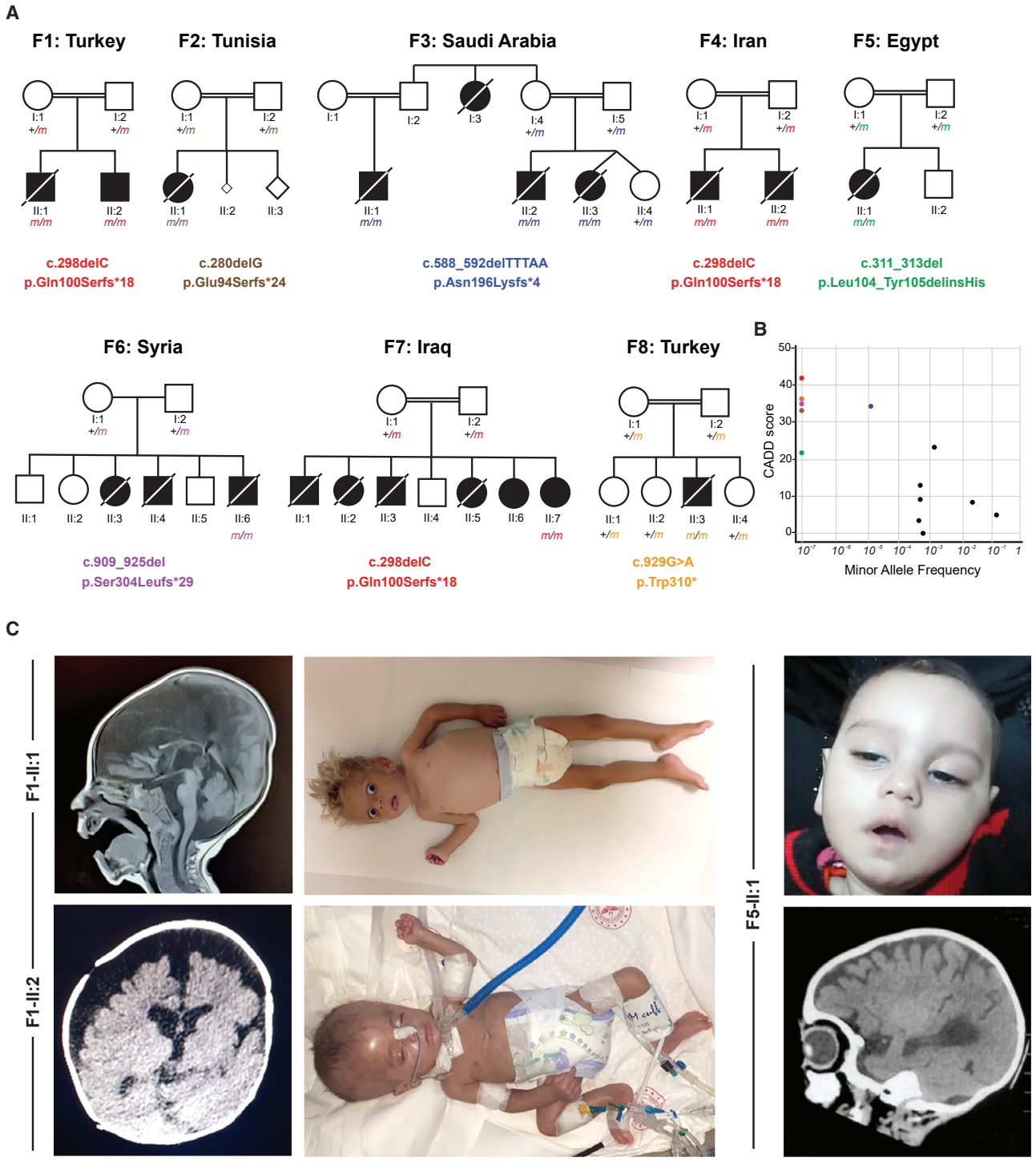

Figure 1. Eight families segregating recessive loss-of-function *C2orf69* germline mutations

(A) Pedigrees of eight consanguineous families segregating homozygous *C2orf69* loss-of-function variants. The identified germline homozygous mutations are shown for 12 affected individuals; eight additional children with similar symptoms died before they could be tested.

(B) *C2orf69* is intolerant of genetic variation. Minor allele frequency (MAF) and combined annotation-dependent depletion (CADD) score of homozygous C2orf69 coding variants found in gnomAD v.2.1.1 (black dots) and those found in each family (color-coded dots).

(C) Photographs and brain MRIs taken at 10 months of age (F1-II:1), 5 months of age (F1-II:2), and 6 months of age (F5-II:1) showing cerebral atrophy with leukoencephalopathy.

Table 1. Abridged clinical presentation of 12 children with homozygous loss-of-function *C2orf69* variants causing Elbracht-Işikay syndrome

	Family 1		Family 2	Family 3			Family 4		Family 5	Family 6	Family 7	Family 8
Individual	II:1	II:2	II:1	II:1	II:2	II:3	II:1	II:2	II:1	II:6	II:7	II:3
Origin	Turkey	Turkey	Tunisia	Saudi Arabia			Iran		Egypt	Syria	Iraq	Turkey
Sex	male	male	female	male	male	female	male	male	female	male	female	male
C2orf69 variant (GenBank: NM_153689.5)	c.298delC		c.280delG	c.588_592delTTTAA			c.298delC		c.311_313del	c.909_925del	c.298delC	c.929G>A
Predicted/observed protein change (UniProt: Q8N8R5)	p.Gln100Serfs*18/p.0		p.Glu94Serfs*24/NT	p.Asn196Lysfs*4/NT			p.Gln100Serfs*18/p.0		p.Leu104_Tyr105delinsHis/NT	p.Ser304Leufs*29/NT	p.Gln100Serfs*18/p.0	p.Trp310*/NT
Clinical synopsis												
Disease onset	3 months	3 months	congenital	NA	NA	congenital	3 months	4 months	2 months	4 months	neonatal	neonatal
Head circumference at birth (cm)	normal	NA	35	NA	NA	NA	normal	normal	33 (−0.6 SD)	normal	NA	35 (−0.4 SD)
Birth weight (kg)/ birth length (cm)	3.75/ normal	2.3/45	3.1/50	NA	NA	2.12/NA	3.5/52	3.7/50	3.0/49	3.5/normal	3.5/NA	3.1/49
Age at last exam (month)/head circumference (cm)	12/39 (−5 SD)	6/39 (−3.1 SD)	18/39.5 (−6 SD)	NA	NA	6/36 (−6 SD)	24/NA	NA	6/37 (−3.5 SD)	6/NA	6/NA	7/37 (−5.5 SD)
Failure to thrive (weight at last exam [kg]) (HP: 0001508)	+ (4.9, −5.3 SD)	+ (4.3, −4.3 SD)	+ (6.5, −3 SD)	NA	NA	+ (4.6)	+	NA	+ (4.7, −3.25 SD)	+ (2.5, −5 SD)	+	+ (5.8, −3 SD)
Post-natal short stature (length at last exam [cm]) (HP: 0004322)	+ (68, −2.7 SD)	+ (58, −3.7 SD)	+ (85)	NA	NA	+ (53)	NA	NA	+ 59 (−3.4 SD)	NA	+	+ (60, −3.5 SD)
Deceased (age of death)	+ (18 months)	alive (in critical condition)	+ (32 months)	+ (NA)	+ (18 months)	+ (24 months)	+ (29 months)	+ (11 months)	+ (9 months)	+ (9 months)	alive (in critical condition)	+ (12 months)
Cause of death	pneumonia	NA	status epilepticus	NA	NA	NA	pneumonia	pneumonia	pneumonia	cardiac arrest	NA	pneumonia
Brain anomalies												
Developmental delay (HP: 0001263)	+	+	+	+	+	+	+	+	+	+	+	+
Secondary microcephaly (HP: 0005484)	+	+	+	+	+	+	NA	NA	+	−	+	+
Dysgenesis of corpus callosum (HP: 0006989)	+	+	−	NA	NA	NA	+	+	+	+	+	−

(*Continued on next page*)

Table 1. ***Continued***

	Family 1		Family 2	Family 3			Family 4		Family 5	Family 6	Family 7	Family 8
CNS hypomyelination (HP: 0003429)	+	+	−	NA	NA	NA	NA	NA	+	+	+	+
Cerebral atrophy (HP: 0002059)	+	+	+	NA	NA	NA	NA	NA	+	+	+	+
Seizures (HP: 0001250)	+	+	+ (focal, pharmacoresistant)	+ (intractable)	+	+ (focal)	+ (absent seizures, several episodes)	NA	+ (myoclonic, several times a day)	+ (tonic)	+ (focal and myoclonic)	+ (intractable, focal)
Immune anomalies												
Recurrent fever (HP: 0001954)	+	+	+	NA	NA	NA	+	+	+	−	+	+
Inflammatory arthritis (HP: 0001369)	−	−	−	NA	NA	NA	+	+	−	−	−	+ (knee, once)
Septic arthritis (HP: 0003095)	−	−	−	NA	NA	NA	+	+	−	−	−	−
Aseptic osteomyelitis (HP: 0002754)	+ (tibia, elbow, hip)	−	−	NA	NA	NA	+ (elbows, hip, clavicle)	NA	−	−	−	−
Elevated C-reactive protein level (HP: 0011227)	+	+	−	NA	NA	NA	+	NA	+	−	−	+
Hypochromic microcytic anemia (HP: 0004840)	+	+	NT	NA	NA	NA	+	NT	+	NA	NA	anemia due to congenital dyserythropoietic anemia
Other phenotypes												
Muscular hypotonia (HP: 0001252)	+	+	+	NA	+	+	−	−	+	+	+	+
General muscle wasting (HP: 0009055)	+	+	+	NA	NA	NA	+	NA	+	+	+	+
Abdominal distention (HP: 0003270)	+	+	−	NA	NA	NA	+	+	NA	−	−	−
Muscular spasticity (HP: 0001257)	−	−	+	NA	NA	NA	+	+	NA	+	NA	−
Hepatomegaly (HP: 0002240)	+	+	−	NA	NA	NA	−	−	−	−	NA	−

Abbreviations are as follows: −, negative; +, affirmative; NT, not tested; NA, not available; CS, caesarean section; NVD, normal vaginal delivery. Additional information on each individual is presented in the supplemental information.

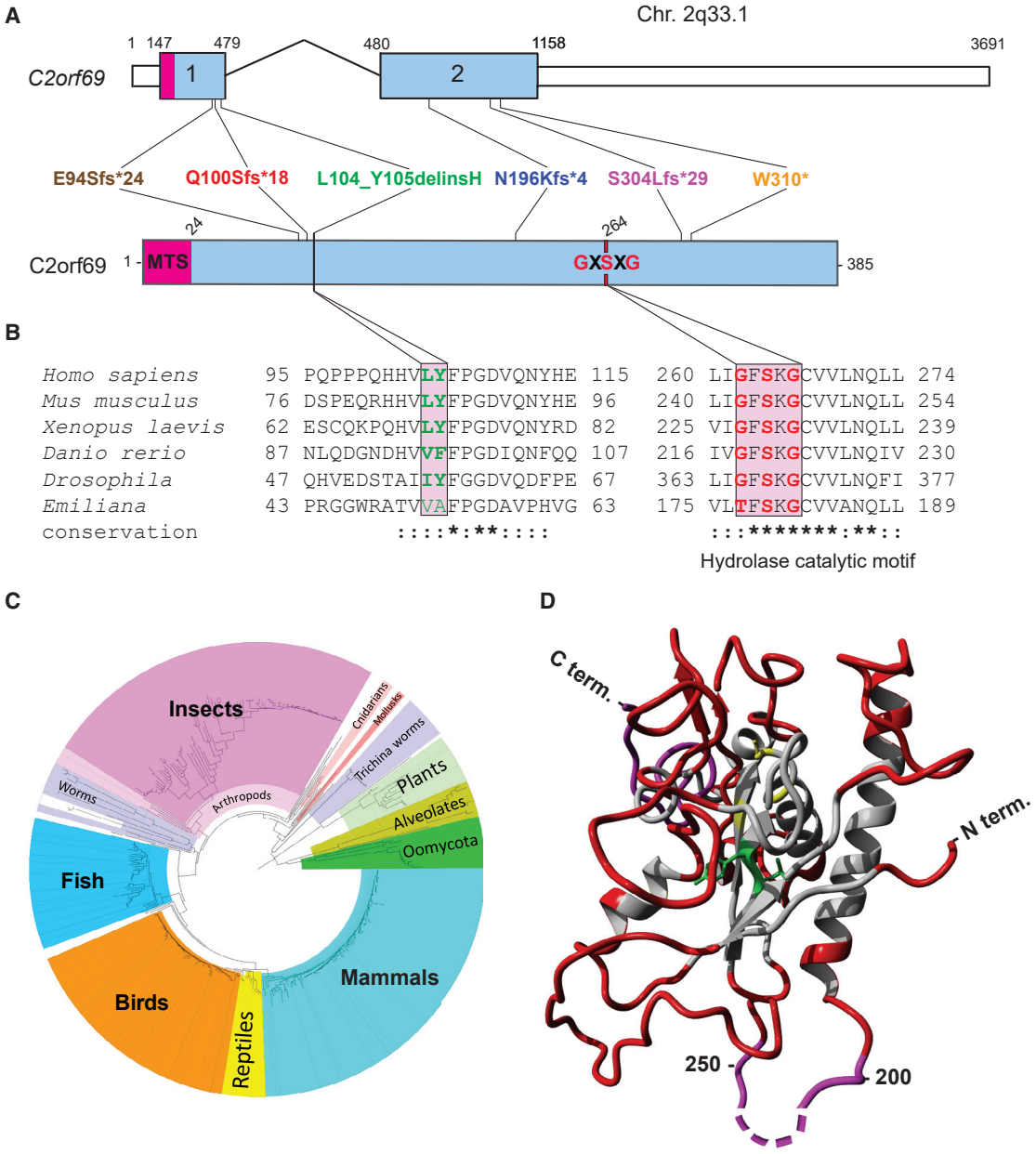

Figure 2. C2ORF69 is conserved in most eukaryotic species and possesses homology to esterase enzymes
(A) Exon-intron genomic organization of *C2orf69* with positions of the six germline loss-of-function mutations identified.
(B) Protein organization of C2orf69 with positions of identified mutations.
(C) Amino acid sequence conservation of C2orf69 orthologs across all major eukaryotic phyla. With the exception of fungi, C2orf69 is recorded in all metazoans, plants, and phytoplankton.
(D) 3D structure prediction of human C2ORF69 with annotated residues L104_Y105 in green and predicted catalytic residue Ser264 in yellow.

C2ORF69 encodes an outer-membrane mitochondria-targeted protein

Automated sequence annotations by UniProt and the Human Protein Atlas indicate that C2ORF69 may contain a secretion signal peptide consistent with extracellular localization. However, the endogenous C2ORF69 in the supernatant of cultured fibroblasts was variable and sometimes undetectable. When overexpressed, a small fraction of the tagged protein could be detected in the cultured media (Figure S1A).

We sought to clarify the subcellular localization of C2ORF69, but available antibodies could not detect the endogenous protein by immunofluorescence. Therefore, we expressed the open-reading frame with a FLAG tag at its C terminus in human fibroblasts. The tagged protein was found to be in close proximity to mitochondria, as revealed by co-localization with MitoTracker Red CMXRos (Figure 3A). Next, we performed cell fractionation by using primary human fibroblasts and obtained a major cytosolic localization and a minor fraction of endogenous C2ORF69

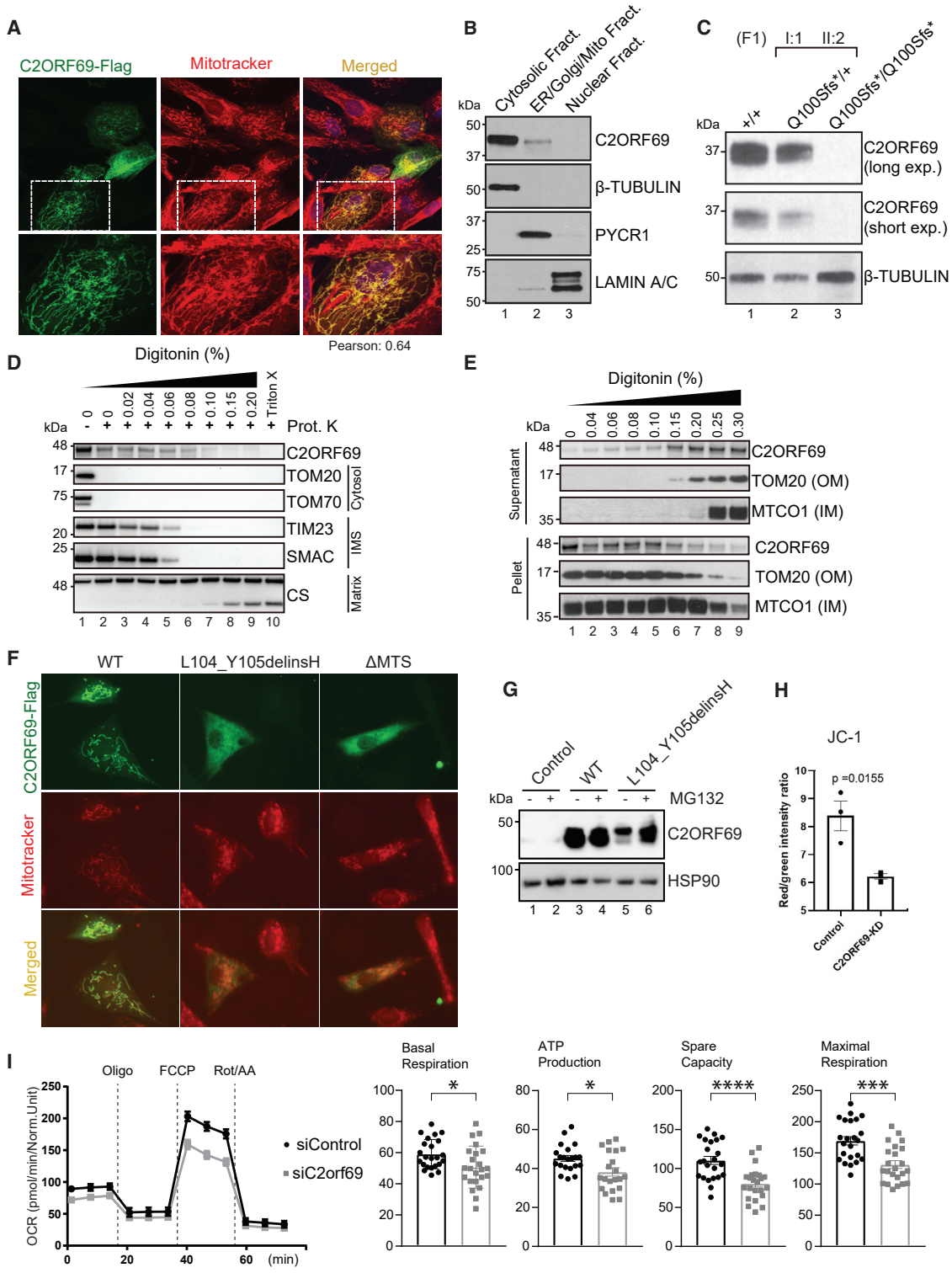

Figure 3. C2ORF69 associates with mitochondria and affects oxidative respiration of neurons

(A) Immunostaining of BJ-TERT fibroblasts overexpressed with C2ORF69-FLAG with FLAG antibodies (green) revealed co-localization with mitochondria marker, MitoTracker CXMRos (red). Pearson's correlation coefficient was analyzed with Fiji software.

(B) Cellular fractionation of primary fibroblasts indicates that endogenous C2ORF69 is mostly cytoplasmic, but a small fraction is associated with membranous fractions including mitochondria.

(C) C2ORF69 protein is absent in primary dermal fibroblast with the homozygous p.Gln100Serfs*18 variant.

(D) Proteinase K protection assay of HEK293T mitochondria to reveal topology and submitochondrial location of endogenous C2ORF69. The majority of the protein resides in the outer membrane vulnerable to proteinase K, and a small fraction displays evidence of translocation into the mitochondria. IMS, intermembrane space.

(legend continued on next page)

with the mitochondrial and ER/Golgi membranes (Figure 3B, lanes 1–3). This result was not changed in fibroblasts that are deficient for MTX1 and MTX2,[5] two proteins involved in the translocation of nuclear-encoded proteins into the outer mitochondrial membrane (OMM) (Figure S1B, lanes 4–6). The specificity of the commercial antibody was validated with cellular extracts of primary dermal fibroblasts obtained from the heterozygous mother (F1-I:1) and her affected son (F1-II:2), which showed that the p.Gln100Serfs*18 variant results in a protein null allele (Figure 3C). To determine the topology and localization of mitochondrial-associated C2ORF69, we treated HEK293T mitochondrial extracts with proteinase K in the presence of increasing concentrations of digitonin. This revealed that the majority of C2ORF69 is associated with the OMM, facing the cytosolic side, as evidenced by the susceptibility of C2ORF69 to proteinase K in the absence of digitonin (Figure 3D, lane 1 versus lane 2). However, a minority of C2ORF69 displays evidence of import into the intermembrane space (IMS) (Figure 3D, lanes 3–5) with traces detectable even in the matrix (Figure 3D, lanes 6–9). Compared to OMM integral membrane proteins such as TOM20, C2ORF69 can be extracted by the lowest digitonin concentrations (Figure 3E), suggesting that it is not inserted into the OMM and remains primarily associated with the OMM on the cytosolic face. The low cytosolic signal observed by immunofluorescence suggests that most of the protein is loosely associated with mitochondrial membranes and may dissociate during cell fractionation (Figure 3B). Alternatively, the protein may primarily reside in the cytosol and become selectively trafficked to the mitochondrion.

Importantly, overexpression of the proband-derived p.Leu104_Tyr105delinsHis variant resulted in the loss of mitochondrial targeting, as did the deletion of the predicted mitochondrial targeting or association signal (MTS) (Figure 3F). By immunoblot, we noted that the p.Leu104_Tyr105delinsHis mutant protein was present at a much lower level than its WT counterpart (Figure 3G, lane 3 versus lane 5). This most likely reflects decreased protein stability because addition of MG132, a proteasomal inhibitor, could readily rescue its half-life to WT levels (Figure 3G, lane 5 versus lane 6). These results indicate that this indel mutation is most likely a bona fide loss-of-function variant that disrupts the structure of C2ORF69, rendering the protein unstable and targeting it for proteasome-mediated degradation. These cellular and molecular results, which are congruent with those reported in children with highly deleterious truncating variants, are consistent with the phenotype observed in subject II:1 of family 5.

C2ORF69 depletion affects mitochondrial respiration

Epileptic seizures are a cardinal feature of mitochondrial diseases caused by mutations in mtDNA and nuclear-encoded mitochondrial genes.[14] We next investigated the effects of C2ORF69 depletion on mitochondrial activity in primary fibroblasts by using siRNA-mediated knockdown of endogenous C2ORF69 (Figure S1C). *C2orf69* knockdown (KD) did not overtly impair respiration (Figure S1D) but led to slightly reduced membrane potential (Figure S1E). Concurrently, the production of mitochondrial reactive oxygen species (mitoROS), as assayed by mitochondrial-targeted redox-sensitive dye mitoSOX, was significantly elevated (Figure S1F). Since the probands' phenotypes largely manifest in the CNS, we reasoned that neurons are a more relevant cell lineage to address the etiology of this disease. We differentiated neuronal progenitors ReNcell VM into neurons and again depleted C2ORF69 by using siRNA (Figure S1G). On the other hand, mitochondrial membrane potential was significantly affected as measured by the ratiometric potential-sensitive JC-1 dye[27] (Figure 3H, Figure S1H). A potential caveat is that JC-1 is sensitive to H_2O_2 levels, such that the observed results could be partially due to increased ROS production in siC2ORF69 neurons. The observed attenuation in mitochondrial membrane potential resulted in significantly reduced oxidative respiration in siC2ORF69 neurons (Figure 3I). Overall, these data suggest a mitochondrial defect that is cell type specific and more pronounced in neuronal lineages.

With fatal seizures, *C2orf69* knockout zebrafish phenocopy human syndrome

To better understand the physiological role of C2orf69, we set out to engineer knockout zebrafish by using CRISPR-Cas9 technology. Through the use of two gRNAs targeting exon 1 of the zebrafish *C2orf69* ortholog (GenBank: NM_001077728.1, zgc153521), we identified, selected, and outbred two independent germline frameshift alleles: c.112del (p.Thr38Profs*38) and c.207del (p.Asn70Metfs*6) (Figure 4A). qPCR analysis indicated that *C2orf69*

(E) Differential membrane extraction assays in HEK293T mitochondria confirm that endogenous C2ORF69 is both cytosolic and mitochondrial membrane associated.
(F) Immunostaining of BJ-TERT fibroblasts overexpressed FLAG epitope-tagged wild-type (WT) C2ORF69, L104_Y105delinsH, and C2ORF69 without mitochondria-targeting signal (ΔMTS). We immunostained cells with FLAG antibodies (green) and MitoTracker CXMRos (red) to determine co-localization.
(G) Immunoblot of fibroblasts overexpressing wild-type C2ORF69 or L104_Y105delinsH treated with proteasome inhibitor, MG132 (20 μM). Treatment with MG132 rescued expression level of p.Leu104_Tyr105delinsHis to near WT levels.
(H) Ratiometric JC-1 (1 μM) membrane potential measurement in ReN VM neurons. Each dot represents the average of all ratiometric measurements across three separate 40× fields of one well. Data are mean ± SEM, and p value is derived from unpaired t test.
(I) Agilent Seahorse Mito Stress Test on siControl- and siC2orf69-differentiated ReNcell VM neurons with basal respiration, ATP production, maximal respiration rate, and spare values indicated.

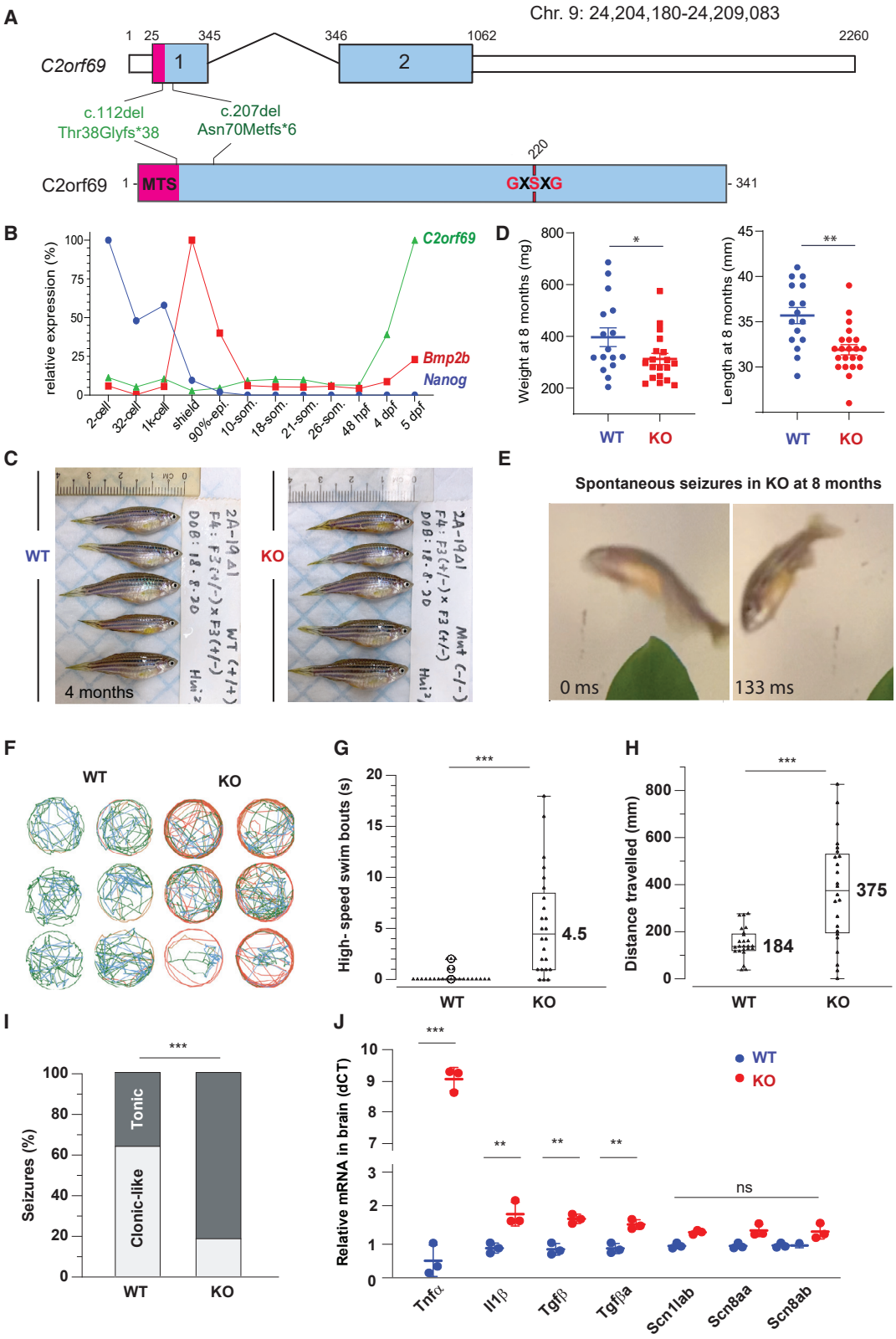

Figure 4. KO *C2orf69* zebrafish phenocopy the human syndrome with spontaneous fatal seizures

(A) Exon-intron structure of the *C2orf69* ortholog in zebrafish. Annotations of the two distinct germline frameshift mutations generated by CRISPR-Cas9 editing at the genome and protein levels.

(B) Developmental expression of *C2orf69* during early zebrafish embryogenesis. The transcription of *C2orf69* begins at 48 hpf without any detectable maternal contribution.

(C) C2orf69 KO fish are indistinguishable from WT siblings at 4 months.

(legend continued on next page)

mRNA is not maternally deposited in the egg (but its protein could be present by virtue of being attached to mitochondria), and a zygotic transcription began by 2 dpf (Figure 4B). Inbreeding of heterozygous mutant fish results in the expected 25% ratio of homozygous knockout animals, which by the age of 4 months, were indistinguishable in size from WT siblings (Figure 4C, Figure S2A). Zygotic null fish could be inbred allowing to produce 100% maternal zygotic (MZ) knockout fish. Whole larval respiration at 36 hours post fertilization (hpf) of MZ knockout embryos was not significantly altered (Figure S2B), possibly reflecting the lineage-specific effects of C2orf69 knockdown observed in human neurons (Figures 3H and 3I). While skeletal muscle mitochondria from adult MZ knockouts did not have gross electron transport chain (ETC) assembly defects as ascertained by BN-PAGE (Figure S2C) and respiratory chain enzymatic assays (Figure S2D), respiratory supercomplexes were mildly attenuated as revealed by in-gel complex I enzymology (Figure S2E). These results indicate that C2ORF69 does not directly impact the integrity of the ETC but nonetheless is required for proper oxidative respiration.

By 8 months of age, MZ knockout fish were significantly smaller both in terms of weight and length (Figure 4D), suggesting a possible growth retardation compared to WT fish. Under normal conditions, we observed that adult *C2orf69*^{Asn70Metfs*3} knockout zebrafish died between 8 to 10 months of spontaneous epileptic seizures (Figure 4E and Video S1). This striking phenotype is reminiscent of the documented seizures seen in children lacking C2orf69. To further verify that mutant fish had increased susceptibility to seizures, we subjected 7- to 11-day-old larva to PTZ, a convulsant shown to induce seizure-like activity in zebrafish.[28] Mutants showed a lower latency to reach stage 2 seizure-like activity (Figure 4F), characterized by frequent high-speed swimming bouts (Figure 4G) and traveling greater distances (Figure 4H) compared to WT larvae. The reduction in latency for induced seizure was also seen in 2- to 3-month-old adults with the same treatment. Mutant adults exhibit tonic seizure-like activity (Video S2) compared to WT siblings, which usually show clonic seizure-like activity (Figure 4I).

To examine whether mutant fish might exhibit tissue damage in the CNS, we collected whole brains from healthy 4-month-old WT and MZ null fish and measured a series of molecular markers by qPCR (Figure 4J). Consistent with sterile CNS inflammation, knockout fish revealed significantly increased expression of *il1β*, *tgfβ*, and *tnfα* (9-fold over WT). Levels of the Nav1.1 voltage-gated sodium channels, *scn1ab*, *scn8aa*, and *scn8ab* were unchanged, suggesting that the disease etiology is distinct from Dravet syndrome (MIM: 607208), another severe pediatric epilepsy syndrome that is successfully modeled in zebrafish.[29] These results obtained in a surrogate animal model reveal that the *in vivo* function of C2orf69 is conserved between mammals and fish and that the product of this gene is essential for brain development and homeostasis in two distantly related vertebrate species.

C2ORF69 inactivation leads to glycogen metabolic defects in humans and zebrafish

A muscle biopsy obtained during the diagnostic work-up of the affected individual (II:3) from family 8 at the age of 5 months revealed some changes suggestive of mitochondrial myopathy, such as subsarcolemmal accumulation of mitochondria and mild cytochrome *c*-oxidase (COX) deficiency (Figures 5A–5D). Although typical ragged-red fibers were not seen in sections stained by modified Gomori trichrome stain, few fibers showed abnormal mitochondrial aggregates (Figure 5B). COX staining was faint in some fibers, better detected by COX-SDH staining (Figure 5D). An intriguing finding was the presence of abnormal granular staining by PAS, which was partially resistant to diastase (amylase), in many fibers (Figures 5E and 5F). Diastase-resistant PAS staining indicates accumulation of polyglucosan bodies, which is pathognomonic for glycogen storage disease type IV (MIM: 232500), caused by defects in glycogen branching enzyme encoded by *GBE1 (*MIM: 607839). A possible relationship between GBE1 and C2ORF69 was also suggested by Kurth and colleagues.[21] We thus generated two independent CRISPR-mediated *C2orf69* KO lines and a *GBE1* KO line in human haploid HAP1 cells. By immunoblot, compared to parental WT cells, endogenous GBE1 levels were decreased by approximately 50% in both *C2orf69* KO lines (Figure 5G, lanes 1 and 2 versus lanes 3 and 4).

Finally, we sought to assess whether polyglucosan bodies could also be seen in KO C2orf69 zebrafish. At 6 months of age, compared to WT siblings, mutant fish displayed sporadic aggregates of PAS-positive staining in skeletal but not cardiac muscles (Figures 5H and 5I). Evident vacuolation was also seen in muscle fibers positive for PAS aggregates in mutant fish. These myocytes appeared

(D) C2orf69 KO fish show statistically significant reduced body mass and length at 8 months.
(E) Spontaneous seizures in adult 8-month-old KO fish lead to fully penetrant lethality.
(F) Six representative swimming tracks extracted from 2 min videos of 11 dpf KO and WT larvae each show high-speed swimming bouts (red) within 5 min of exposure to 5 mM PTZ.
(G) Quantification of high-speed swim bouts in 2 min (n = 24 each). The p value of the two-sided permutation t test is <0.0001
(H) Quantification of distance swam in 2 min (n = 24 each). The p value of the two-sided permutation t test is 0.0008
(I) The percentage of KO adult fish that show tonic seizures upon exposure to 5 mM PTZ (80%) within 12 min is 2.5-fold higher compared to WT (27%). The p value of the two-sided t test is 0.03.
(J) Molecular markers from 4-month-old whole brain extracts measured by qPCR reveal constitutive CNS inflammation in KO adult fish compared to WT siblings.

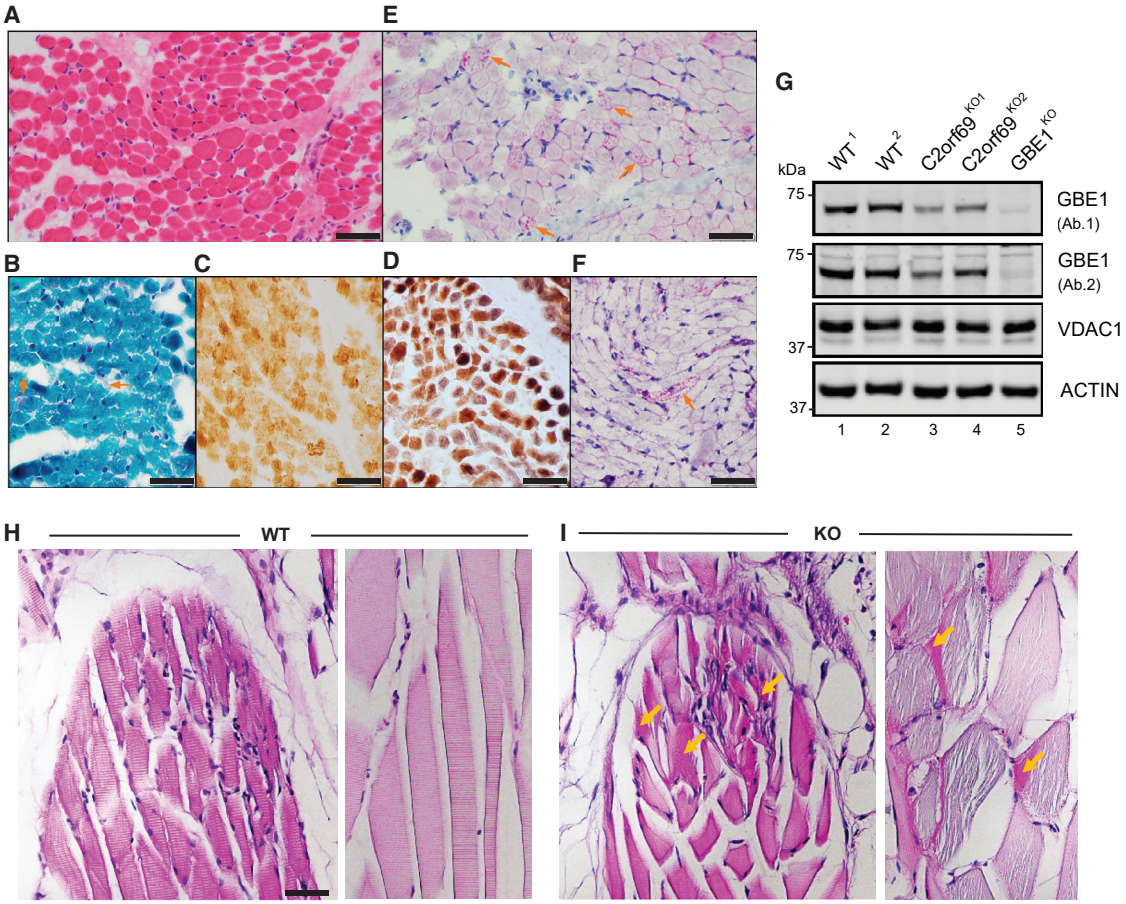

Figure 5. *C2orf69* deficiency leads to the accumulation of glycogen in skeletal muscles
(A) Skeletal muscle biopsy of proband II:3 from family 8 shows mild variation of fiber size in H&E sections.
(B) Subsarcolemmal accumulation of mitochondria is apparent in some fibers (arrows) by modified Gomori-trichrome stain.
(C) Several fibers show faint staining by cytochrome-c-oxidase (COX) stain.
(D) These COX-deficient fibers are more easily identified as bluish fibers by COX-SDH stain.
(E) Periodic acid Schiff (PAS) stain shows unusual granular staining in many fibers (arrows), which are partially resistant to diastase, as seen by PAS-diastase stain (F).
(F) PAS-positive material is seen in a few fibers after diastase treatment. Scale bars represent 50 μm.
(G) Approximately 50% decrease in endogenous GBE1 levels is seen in two independent *C2orf69* KO HAP1 cell lines with two different antibodies (Ab1, Proteintech; Ab2, Abcam). Two WT and *GBE1* KO HAP1 cell lines act as positive and negative controls. Antibodies against VDAC1 and ACTIN are used as loading controls.
(H) PAS stain in skeletal muscles of WT zebrafish at 6 months of age.
(I) PAS-positive aggregates (marked by orange arrows) in skeletal muscles of *C2orf69* KO zebrafish are suggestive of glycogen accumulation. Sarcomeres were partially disorganized in mutant striated muscle fibers. Scale bar represents 50 μm.

disorganized and without a regular striated organization seen in control fish of the same age (Figure 5I). By recapitulating the accumulation of polyglucosan bodies observed in human probands, C2orf69 knockout zebrafish further substantiate a functional link between GBE1-driven glycogen metabolism and C2orf69 deficiency.

Discussion

In summary, we have identified eight unrelated families with autosomal recessive *C2orf69* deficiency, which is characterized by autoimmune defects, failure to thrive, progressive neurodegeneration of the central nervous system, and early demise. A concurrent study has identified a similar condition in eight additional children,[30] which independently confirms our clinical, genetic, and molecular findings.

Using sequence analysis and cellular assays, we demonstrated that the six germline *C2orf69* variants are likely to have deleterious effects at the protein level. In particular, we confirm that the in-frame indel allele identified in the Egyptian family is more likely to compromise the stability and subcellular localization of C2ORF69. *C2orf69* is highly conserved in eukaryotes but not indispensable for all species because fungi were found not to have a orthologous gene. Structural analysis suggests a single globular domain protein with distant homology with bacterial esterases. The protein contains an N-terminal sequence with similarity to a signal peptide and can be detected in supernatants

of high-density cell cultures. However, in most cell culture conditions, the endogenous protein remains cytosolic and associates with the outer mitochondrial membrane. These data suggest that C2ORF69 could be acting on the lipid composition of membranes. The mitochondrial assays suggest a mild perturbation of the electron transport chain and the production of ROS. These anomalies may manifest as knockon effects driven by alterations of the outer mitochondrial membrane.

A combination of hepatic and neurological findings in the *C2orf69* loss-of-function-associated phenotypes indicates a strong clinical suspicion for mitochondriopathy. However, microscopic identification of diastase-resistant PAS staining in the muscle biopsy from the proband of family 8, without any pathogenic variants in *GBE1*, indicated accumulation of polyglucan, which is uncommon for mitochondrial disorders. The clinical presentation of this newly recognized syndrome is indeed a singular combination of the clinically heterogeneous glycogen storage disease type IV and mitochondriopathy. Furthermore, the selective decrease in glycogen branching enzyme protein levels in *C2orf69* knockout HAP1 cells supports a link between GBE1 and C2orf69. An independent study also supports this finding through a combination of biopsy findings from heart, muscle, and liver tissues and a decrease in GBE1 enzymatic activity.[21] Whether C2orf69's control over GBE1 is caused by a decrease in expression or increased degradation and how they link the two important energy metabolism-related processes in the cell, glycogen synthesis, and OXPHOS still needs to be addressed. Therefore, this intertwined phenotype is particularly challenging for pathological diagnosis of mitochondriopathies because muscle biopsy samples are commonly obtained for assessment of mitochondrial activity but findings about glycogen storage may be overlooked. In particular, a combination of intractable developmental and epileptic encephalopathy, autoinflammatory dysregulation, and hepatic involvement should urge the clinical teams to look for glycogen-storage-related mitochondriopathy.

Despite being ubiquitously expressed, the clinical presentation suggests that specific tissues such as neuronal lineages are particularly affected by C2ORF69 depletion. The protein localization at the mitochondria suggests that the children's symptoms are at least in part due to defective mitochondrial function in neurons and/or glia of the CNS. This notion is supported by *in vivo* experiments where the lethality of *C2orf69* mutant zebrafish was apparently linked to defects in the CNS. Lending credence to the notion that C2ORF69 plays an active role in the development/homeostasis of the immune and central nervous systems, genome-wide association studies (GWASs) have revealed genome-wide significant non-coding variants in the intron of *C2orf69* to be positively associated with susceptibility to chickenpox infections (rs191220855, $p = 3 \times 10^{-7}$)[31] and schizophrenia (rs1658810, $p = 2 \times 10^{-13}$).[32] A subsequent GWAS has found that common C2orf69 variants are associated with eight other neuropsychiatric disorders, such as autism and Tourette syndrome.[32] This was further validated in a transcriptome-wide association study where endogenous *C2orf69* levels were significantly associated with schizophrenia and changes in chromatin architecture.[33] Finally, a genome-wide methylation quantitative trait loci (meQTLs) study also corroborated this finding by demonstrating a cross-tissue genetic-epigenetic effect of *C2orf69* in schizophrenia.[34] Our results and these independent studies implicate that both common and rare *C2orf69* variants contribute to brain and immune malfunction in humans.

The autoinflammation observed in children with Elbracht-Işikay syndrome is not commonly seen with mitochondriopathies. On the other hand, glycogen metabolism has recently been linked to acute inflammatory response in macrophages.[35] Thus, the autoinflammation may be linked to metabolic perturbation in immune cells. The late onset lethality observed in the zebrafish model is a salient difference with the early demise seen in humans. The zebrafish genome does not seem to have other C2orf69 paralogs that could functionally compensate. As C2ORF69 appears involved in bioenergetics, a possible explanation is that tissues of warm-blooded animals, with higher metabolic needs, are more sensitive to the loss of the protein. In addition to these questions, future studies will need to address whether C2ORF69 serves as a bespoke lipase/esterase. If so, efforts will need to be invested to find substrate(s) and enzymatic product(s), the accumulation or absence of which, respectively, may be responsible for the observed autoinflammatory symptoms.

Data and code availability

The data that support the findings of this study are available within the paper or from the corresponding authors upon reasonable request.

Supplemental information

Supplemental information can be found online at https://doi.org/10.1016/j.ajhg.2021.05.003.

Acknowledgments

We thank all the families for partaking in this study and the referring clinicians for their generous help. We are grateful to all members of the Reversade, Ho, and Bard laboratories for swift support. We thank Z. Ekim Taskiran for facilitating WES studies in the Hacettepe University Exome Facility and Can Kosukcu for obtaining WES data. We thank Mohd Agus and the IMCB aquatics facility for zebrafish husbandry. H.H.W. and S.H.S. are supported by a grant from Procter and Gamble. J.L.C. is supported by the Howard Hughes Medical Institute (HHMI), the Rockefeller University, the St. Giles Foundation, Institut National de la Santé et de la Recherche Médicale (INSERM), and the "Université de Paris." S.U. is supported by E-Rare grants for EuroDBA Project (TUBITAK, #315S192). S.Z. is supported by a Khoo Teck Puat postdoctoral fellowship. A.C. is supported by the EU's Horizon 2020 research

and innovation program under the EJP RD COFUND-EJP no. 825575 (TUBİTAK, #319S062). D.J.P. is supported by NIH awards R35 GM131795 and P41 GM108538, a UW2020 award, and funds from the BJC Investigator Program. J.J.C. is supported by NIH awards, P41 GM108538, and a UW2020 award. S.X. is supported by NMRC/OFYIRG/062/2017. A.S.M. and F.M.N. are supported by the Ministry of Education, Singapore and Yale-NUS College (IG19-BG106 and SUG). L.H. is supported by fellowships NRF-NRFF2017-05 and HHMI-IRSP55008732. T.M. is supported by The Uehara Memorial Foundation. D.P. is supported by International Rett Syndrome Foundation (#3701-1). J.R.L. is supported by the National Human Genome Research Institute, the National Heart, Lung, and Blood Institute, The Baylor-Hopkins Center for Mendelian Genomics (#HG006542), and the National Institutes of Neurological Disease and Stroke (R35NS105078) and Muscular Dystrophy Association (#512848). B.R. is an investigator of the National Research Foundation (Singapore) and is supported by a use-inspired basic research grant from the Agency for Science & Technology and Research (A*STAR) in Singapore.

Declaration of interests

J.R.L. has stock ownership in 23andMe and is a paid consultant for the Regeneron Genetics Center. The Department of Molecular and Human Genetics at Baylor College of Medicine receives revenue from clinical genetic testing conducted at Baylor Genetics (BG) Laboratories. J.R.L. serves on the Scientific Advisory Board of BG. A.B.A. and P.B. are employees of CENTOGENE GmbH. S.C. is a shareholder of Intergen Genetic Diagnosis Center. J.J.C. is a consultant for Thermo Fisher Scientific. All other authors declare no competing interests.

Received: March 19, 2021
Accepted: May 7, 2021
Published: May 25, 2021; Corrected online: June 16, 2021

Web resources

1000 Genomes Project Database, https://www.internationalgenome.org/
CENTOGENE, https://www.centogene.com/downloads
CRISPRScan, https://www.crisprscan.org/
Exome Aggregation Consortium (ExAC), http://exac.broadinstitute.org
GenBank, https://www.ncbi.nlm.nih.gov/genbank/
gnomAD, https://gnomad.broadinstitute.org/
Greater Middle East (GME) Variome, http://igm.ucsd.edu/gme/index.php
NCBI dbSNP, https://www.ncbi.nlm.nih.gov/SNP/
OMIM, https://omim.org
The Exome Variant Server (ftp://ftp.ncbi.nlm.nih.gov/pub/clinvar/vcf_GRCh37) from NHLBI Exome Sequencing Project (ESP), https://evs.gs.washington.edu/EVS/

References

1. Song, J., Herrmann, J.M., and Becker, T. (2021). Quality control of the mitochondrial proteome. Nat. Rev. Mol. Cell Biol. *22*, 54–70.
2. Gorman, G.S., Chinnery, P.F., DiMauro, S., Hirano, M., Koga, Y., McFarland, R., Suomalainen, A., Thorburn, D.R., Zeviani, M., and Turnbull, D.M. (2016). Mitochondrial diseases. Nat. Rev. Dis. Primers *2*, 16080.
3. Nunnari, J., and Suomalainen, A. (2012). Mitochondria: in sickness and in health. Cell *148*, 1145–1159.
4. Tein, I., Demaugre, F., Bonnefont, J.P., and Saudubray, J.M. (1989). Normal muscle CPT1 and CPT2 activities in hepatic presentation patients with CPT1 deficiency in fibroblasts. Tissue specific isoforms of CPT1? J. Neurol. Sci. *92*, 229–245.
5. Elouej, S., Harhouri, K., Le Mao, M., Baujat, G., Nampoothiri, S., Kayserili, H., Menabawy, N.A., Selim, L., Paneque, A.L., Kubisch, C., et al. (2020). Loss of MTX2 causes mandibuloacral dysplasia and links mitochondrial dysfunction to altered nuclear morphology. Nat. Commun. *11*, 4589.
6. Narendra, D., Tanaka, A., Suen, D.-F., and Youle, R.J. (2009). Parkin-induced mitophagy in the pathogenesis of Parkinson disease. Autophagy *5*, 706–708.
7. Escande-Beillard, N., Loh, A., Saleem, S.N., Kanata, K., Hashimoto, Y., Altunoglu, U., Metoska, A., Grandjean, J., Ng, F.M., Pomp, O., et al. (2020). Loss of PYCR2 Causes Neurodegeneration by Increasing Cerebral Glycine Levels via SHMT2. Neuron *107*, 82–94.e6.
8. Calvo, S.E., Clauser, K.R., and Mootha, V.K. (2016). MitoCarta2.0: an updated inventory of mammalian mitochondrial proteins. Nucleic Acids Res. *44* (D1), D1251–D1257.
9. Calvo, S.E., and Mootha, V.K. (2010). The mitochondrial proteome and human disease. Annu. Rev. Genomics Hum. Genet. *11*, 25–44.
10. Macdonald, R., Barnes, K., Hastings, C., and Mortiboys, H. (2018). Mitochondrial abnormalities in Parkinson's disease and Alzheimer's disease: can mitochondria be targeted therapeutically? Biochem. Soc. Trans. *46*, 891–909.
11. Fecher, C., Trovò, L., Müller, S.A., Snaidero, N., Wettmarshausen, J., Heink, S., Ortiz, O., Wagner, I., Kühn, R., Hartmann, J., et al. (2019). Cell-type-specific profiling of brain mitochondria reveals functional and molecular diversity. Nat. Neurosci. *22*, 1731–1742.
12. Rangaraju, V., Lewis, T.L., Jr., Hirabayashi, Y., Bergami, M., Motori, E., Cartoni, R., Kwon, S.-K., and Courchet, J. (2019). Pleiotropic Mitochondria: The Influence of Mitochondria on Neuronal Development and Disease. J. Neurosci. *39*, 8200–8208.
13. Joshi, A.U., Minhas, P.S., Liddelow, S.A., Haileselassie, B., Andreasson, K.I., Dorn, G.W., 2nd, and Mochly-Rosen, D. (2019). Fragmented mitochondria released from microglia trigger A1 astrocytic response and propagate inflammatory neurodegeneration. Nat. Neurosci. *22*, 1635–1648.
14. Zsurka, G., and Kunz, W.S. (2015). Mitochondrial dysfunction and seizures: the neuronal energy crisis. Lancet Neurol. *14*, 956–966.
15. Moehlman, A.T., and Youle, R.J. (2020). Mitochondrial Quality Control and Restraining Innate Immunity. Annu. Rev. Cell Dev. Biol. *36*, 265–289.
16. Jagadeesh, K.A., Wenger, A.M., Berger, M.J., Guturu, H., Stenson, P.D., Cooper, D.N., Bernstein, J.A., and Bejerano, G. (2016). M-CAP eliminates a majority of variants of uncertain significance in clinical exomes at high sensitivity. Nat. Genet. *48*, 1581–1586.
17. Hengel, H., Bosso-Lefèvre, C., Grady, G., Szenker-Ravi, E., Li, H., Pierce, S., Lebigot, É., Tan, T.-T., Eio, M.Y., Narayanan, G., et al. (2020). Loss-of-function mutations in UDP-Glucose 6-Dehydrogenase cause recessive developmental epileptic encephalopathy. Nat. Commun. *11*, 595.

18. Pena, I.A., Roussel, Y., Daniel, K., Mongeon, K., Johnstone, D., Weinschutz Mendes, H., Bosma, M., Saxena, V., Lepage, N., Chakraborty, P., et al. (2017). Pyridoxine-Dependent Epilepsy in Zebrafish Caused by Aldh7a1 Deficiency. Genetics *207*, 1501–1518.
19. Kalueff, A.V., and Stewart, A.M. (2012). Zebrafish Protocols for Neurobehavioral Research (Humana Press).
20. Gaspar, B.L., Vasishta, R.K., and Radotra, B.D. (2018). Myopathology: A Practical Clinico-pathological Approach to Skeletal Muscle Biopsies (Springer).
21. Zhang, S., Reljić, B., Liang, C., Kerouanton, B., Francisco, J.C., Peh, J.H., Mary, C., Jagannathan, N.S., Olexiouk, V., Tang, C., et al. (2020). Mitochondrial peptide BRAWNIN is essential for vertebrate respiratory complex III assembly. Nat. Commun. *11*, 1312.
22. Spinazzi, M., Casarin, A., Pertegato, V., Salviati, L., and Angelini, C. (2012). Assessment of mitochondrial respiratory chain enzymatic activities on tissues and cultured cells. Nat. Protoc. *7*, 1235–1246.
23. Schindelin, J., Arganda-Carreras, I., Frise, E., Kaynig, V., Longair, M., Pietzsch, T., Preibisch, S., Rueden, C., Saalfeld, S., Schmid, B., et al. (2012). Fiji: an open-source platform for biological-image analysis. Nat. Methods *9*, 676–682.
24. Jha, P., Wang, X., and Auwerx, J. (2016). Analysis of Mitochondrial Respiratory Chain Supercomplexes Using Blue Native Polyacrylamide Gel Electrophoresis (BN-PAGE). Curr. Protoc. Mouse Biol. *6*, 1–14.
25. Maurer-Stroh, S., Koranda, M., Benetka, W., Schneider, G., Sirota, F.L., and Eisenhaber, F. (2007). Towards complete sets of farnesylated and geranylgeranylated proteins. PLoS Comput. Biol. *3*, e66.
26. Gabler, F., Nam, S.-Z., Till, S., Mirdita, M., Steinegger, M., Söding, J., Lupas, A.N., and Alva, V. (2020). Protein Sequence Analysis Using the MPI Bioinformatics Toolkit. Curr. Protoc. Bioinformatics *72*, e108.
27. Garner, D.L., and Thomas, C.A. (1999). Organelle-specific probe JC-1 identifies membrane potential differences in the mitochondrial function of bovine sperm. Mol. Reprod. Dev. *53*, 222–229.
28. Baraban, S.C., Taylor, M.R., Castro, P.A., and Baier, H. (2005). Pentylenetetrazole induced changes in zebrafish behavior, neural activity and c-fos expression. Neuroscience *131*, 759–768.
29. Baraban, S.C., Dinday, M.T., and Hortopan, G.A. (2013). Drug screening in Scn1a zebrafish mutant identifies clemizole as a potential Dravet syndrome treatment. Nat. Commun. *4*, 2410.
30. Lausberg, E., Gießelmann, S., Dewulf, J.P., Wiame, E., Holz, A., Salvarinova, R., et al. (2021). A human multisystem disorder with autoinflammation, leukoencephalopathy and hepatopathy is caused by mutations in C2orf69. J. Clin. Invest. https://doi.org/10.1172/JCI143078.
31. Tian, C., Hromatka, B.S., Kiefer, A.K., Eriksson, N., Noble, S.M., Tung, J.Y., and Hinds, D.A. (2017). Genome-wide association and HLA region fine-mapping studies identify susceptibility loci for multiple common infections. Nat. Commun. *8*, 599.
32. Cross-Disorder Group of the Psychiatric Genomics Consortium (2019). Genomic Relationships, Novel Loci, and Pleiotropic Mechanisms across Eight Psychiatric Disorders. Cell *179*, 1469–1482.e11.
33. Gusev, A., Mancuso, N., Won, H., Kousi, M., Finucane, H.K., Reshef, Y., Song, L., Safi, A., McCarroll, S., Neale, B.M., et al.; Schizophrenia Working Group of the Psychiatric Genomics Consortium (2018). Transcriptome-wide association study of schizophrenia and chromatin activity yields mechanistic disease insights. Nat. Genet. *50*, 538–548.
34. Lin, D., Chen, J., Perrone-Bizzozero, N., Bustillo, J.R., Du, Y., Calhoun, V.D., and Liu, J. (2018). Characterization of cross-tissue genetic-epigenetic effects and their patterns in schizophrenia. Genome Med. *10*, 13.
35. Ma, J., Wei, K., Liu, J., Tang, K., Zhang, H., Zhu, L., Chen, J., Li, F., Xu, P., Chen, J., et al. (2020). Glycogen metabolism regulates macrophage-mediated acute inflammatory responses. Nat. Commun. *11*, 1769.

The American Journal of Human Genetics, Volume *108*

Supplemental information

Loss of C2orf69 defines a fatal autoinflammatory syndrome in humans and zebrafish that evokes a glycogen-storage-associated mitochondriopathy

Hui Hui Wong, Sze Hwee Seet, Michael Maier, Ayse Gurel, Ricardo Moreno Traspas, Cheryl Lee, Shan Zhang, Beril Talim, Abigail Y.T. Loh, Crystal Y. Chia, Tze Shin Teoh, Danielle Sng, Jarred Rensvold, Sule Unal, Evgenia Shishkova, Ece Cepni, Fatima M. Nathan, Fernanda L. Sirota, Chao Liang, Nese Yarali, Pelin O. Simsek-Kiper, Tadahiro Mitani, Serdar Ceylaner, Ozlem Arman-Bilir, Hamdi Mbarek, Fatma Gumruk, Stephanie Efthymiou, Deniz Uğurlu Çimen, Danai Georgiadou, Kortessa Sotiropoulou, Henry Houlden, Franziska Paul, Davut Pehlivan, Candice Lainé, Guoliang Chai, Nur Ain Ali, Siew Chin Choo, Soh Sok Keng, Bertrand Boisson, Elanur Yılmaz, Shifeng Xue, Joshua J. Coon, Thanh Thao Nguyen Ly, Naser Gilani, Dana Hasbini, Hulya Kayserili, Maha S. Zaki, Robert J. Isfort, Natalia Ordonez, Kornelia Tripolszki, Peter Bauer, Nima Rezaei, Simin Seyedpour, Ghamar Taj Khotaei, Charles C. Bascom, Reza Maroofian, Myriam Chaabouni, Afaf Alsubhi, Wafaa Eyaid, Sedat Işıkay, Joseph G. Gleeson, James R. Lupski, Jean-Laurent Casanova, David J. Pagliarini, Nurten A. Akarsu, Sebastian Maurer-Stroh, Arda Cetinkaya, Aida Bertoli-Avella, Ajay S. Mathuru, Lena Ho, Frederic A. Bard, and Bruno Reversade

Supplemental Data

Supplemental Note: Case Reports

Family 1 from Turkey

The proband is a 1-year-old male who was presented to the pediatric neurology division due to fussiness, constant crying, low tone and unable to hold his head up. He was born at 41 gestational weeks via normal spontaneous vaginal delivery. Pregnancy was uneventful but he was stained with meconium at birth. He cried soon after delivery. Birth weight was 3750 g (65%ile). His development in the first 3 months were unremarkable, smiled at 2 months and had head control at 3 months. He started progressive deterioration in developmental steps starting at 3 months. His hair color became lighter, his belly became more prominent since the last 4-5 months. He was having frequent hospitalizations due to lung infection and periodic fevers.

In addition to lung infections he had a history of tibia, wrist and hip osteomyelitis requiting hospitalizations and long treatments, He had generalized tonic clonic seizures which were under control with phenobarbital and levetiracetam. He died at the age of 18 months due to aspiration pneumonia while being hospitalized for lung infection.

Anthropometric parameters at 1-year-old revealed weight 4.9 kg (-5.3 SD), height: 68 cm (-2.7 SD) and head circumference: 39 cm (-5.8 SD). Physical examination showed severely delayed with no head control. He had dysmorphic facial features including frontal bossing, thin and long philtrum, broad nasal bridge, large tongue, blonde kinky hair. Abdomen was protuberant and the liver was palpable at 4-5 cm below the lower costal ridge. Light microscopic evaluation of the hair showed brittle, hypopigmented hair with varying diameters. Brain MRI revealed severe global atrophy, diffuse white matter hypomyelination, dystrophic and thin appearing corpus callosum and Dandy-Walker malformation. Ophthalmic evaluation showed optic atrophy.

The proband had an 18 months younger brother born at 36 gestational week via normal spontaneous vaginal delivery, with a birth weight of 2.3 kg (12%ile), height of 45 cm (18%ile). Pregnancy was complicated by polyhydramnios. He was loose since birth and had frequent lung infections and fever episodes. He started having seizures at 2 months of life which was under control with low dose levetiracetam. He has a history of cardiac arrest at 3 months of life. In one of his admissions, his hemoglobin was 7 mg/dl requiring erythrocyte transfusion. He was evaluated at 6 months during one of his hospital admissions due to infection. He was hospitalized most of his life. Growth parameters showed weight 4.3 kg (-4.3 SD), height: 58 cm (-3.7 SD) and head circumference: 39.5 cm (-3.1 SD). He was intubated. Physical evaluated revealed hypotonia, decreased spontaneous movements. Had facial dysmorphia similar to brother but exam was limited due to intubation (frontal bossing and hair type was similar). Hair was sparse, thin, brittle. He had malnutrition, decreased subcutaneous fat, hepatomegaly of 4 cm. Eye examination showed optic atrophy.

Brain CT showed diffuse atrophy and thin corpus callosum. He has multiple increased blood levels of C-reactive protein and lactate.

Informed consent was provided according to the Baylor-Hopkins Center for Mendelian Genomics Research Protocol (IRB number: H-29697). Trio exome (I.1, I.2 and II.1) sequencing was performed as previously described [17]. Validation and segregation of the identified variant in all family members were performed by Sanger sequencing using primers flanking the mutation (Forward: 5'-GCTGCTTGATGGGAACCTAC-3'; Reverse 5'-GCTTGTTTTCTCCCAAAAATG-3') .Primary skin cells were obtained from punch skin biopsies performed on I:1 and II:2.

Family 2 from Tunisia

The index was a 1-year-old female, born to first degree consanguineous Tunisian healthy parents. There is no family history of a similar disease. Pregnancy and delivery were uneventful. The index was born by c-section at term for circular cord. Her birth weight was of 3.1 kg, her height birth height was of 50 cm and her head circumference at birth was of 35 cm. She presented weak sucking at birth. She had global and severe developmental delay with hold up of the head at the age of 18 months. At the age of 8 months, she developed focal seizures with chewing, eye lid and hemicorporeal clonies. The EEG showed a slow background with generalized discharges. She was initially treated by valproate until 40 mg/kg/day without improvement (3 times a week). The phenobarbuital was associated with worsening of seizure hence it was stopped and replaced by levetiracetam until 50 mg/kg/day with decrease of seizures but recurrence when infectious episodes.

Neurological examination at the age of 18 months showed a poor contact, no ocular pursuit, language delay, microcephaly (37.5cm; -6SD), axial hypotonia and spastic tetraparesis. General examination noted failure to thrive (weight was of 6.5kg (-3SD) and height was of 85 cm) abnormal facial shape, narrow forehead, hypertelorism and stereotypy. Fundus examination showed neither optic atrophy nor corneal deposits. Brain MRI concluded to cortical and subcortical atrophy. Spectroscopy was normal. CT scan showed no calcifications. Laboratory tests were normal and CSF analysis were normal. Visual evoked potential, electroretinogram and electro-neuromyogram were normal. Metabolic screening (lactate, chromatographies of amino acids and organic acids) were normal. She passed away at the age of 32 months due to status epilepticus.

Informed consents were provided, including consent for scientific publication. The form contains a section for consent for genetic testing related to the disease(s) of the individual, and consent for research (related to the main concern, but implicating genes not yet associated with human diseases). The informed consent form is available upon request with Centogene. Exome and genome sequencing were performed as previously described [18,19].

Family 3 from Saudi Arabia

The index is a 6-month-old female born to consanguineous parents from Saudi Arabia. Family history is positive, a sibling died at 18 months of age with a history of seizure, hypotonia, ventilator dependent and optic atrophy. The index and her twin sister were born by c-section at 36 weeks of gestation. Her Apgar scores were 6 and 8, and birth weight of 2.1 kg. She required active resuscitation and was admitted to the NICU for two weeks. She was noted to have hypotonia and club foot and presented focal seizures. On physical examination (6 month old), all growth parameters were below the 5th percentile for age and gender (height: 53 cm, weight, 4.6 kg, HC:36 cm). She presented hypotonia, and required mechanical ventilation (under sedation). She had fair, brittle hair and facial dysmorphism: narrow forehead, hypoplastic supraorbital ridge, upturned nostril, micrognathia, and depressed nasal bridge. Her twin sister did not present any abnormality. Her brother is similarly affected and presented neurodevelopmental delay, seizures and hypoplastic corpus callosum and cerebellum. Her male cousin was also affected, he had neurodevelopmental delay and intractable seizures. All affected subjects passed away.

Informed consents were provided, including consent for scientific publication. The form contains a section for consent for genetic testing related to the disease(s) of the individual, and consent for research (related to the main concern, but implicating genes not yet associated with human diseases). The informed consent form is available upon request with Centogene. Exome and genome sequencing were performed as previously described [18,19].

Family 4 from Iran

Chief complaint/ First clinical manifestation:
Fever, Recurrent septic arthritis, sepsis

Present illness and past medical history:
He was a two-year-old boy, from a consanguineous marriage, with no complications during the prenatal and delivery process. He was referred to our center following fever, recurrent septic arthritis, neuromuscular disorders (CP), developmental delay, weaknesses, and sepsis. He was repeatedly hospitalized with FUO (fever of unknown origin) which had a poor response to antibiotic treatment. At 19 months old His mother noticed the limited range of motion in babies' left hip and inflammation in his left elbow. The neuromuscular examinations revealed: a limited range of motion in the left elbow and hips, muscular Spasticity in four limbs, and positive bilateral Babinski in favor of Quadriparetic Cerebral palsy (CP). He also had experienced several episodes of absence seizures. (The brain MRI and EEG report are not available). The Pelvic radiography demonstrated left hip dislocation without dysplasia, suggestive of being secondary to trauma or osteomyelitis. The left hip was reduced with surgical technique and a Pavlik harness was implemented. The left elbow was tapped but had no fluid. Tissue smear and culture were negative for common pathogenic bacteria. The laboratory examinations rolled out HIV, TB, EBV, and brucellosis infection. Regarding the recent antibiotic administration, he was diagnosed with septic arthritis, treated with antibiotics for three weeks at the hospital, and discharged with oral antibiotics (Cefixime, Rifampin, and Clindamycin). He was repeatedly hospitalized with elbows and hips septic arthritis from 18 to 22 months old and underwent several surgical interventions (including elbow abscess drainage, hip fistulectomy, and debridements) as well as antibiotic treatment. Regarding recurrent infections, the patient was investigated for suspected immunodeficiency. He had completed vaccination with no adverse effect, no lymphadenopathy, no organomegaly, no leukopenia, no neutropenia, normal NBT, no complement deficiency, normal flow cytometry, a decreased IgA level (3 months-old and 21 months old), the normal response of specific antibody for tetanus-diphtheria. Unfortunately, the patient had passed away at two years and five-month-old due to sepsis following pneumonia. Family history: The parents are first cousins and the patient's sibling had passed away at 11 months old. He had similar symptoms including recurrent infections, arthritis, neuromuscular disorders (CP), and development retardation, and finally died following severe pneumonia. The parents did not recall a similar case in other relatives. Presently they have no other children and the mother had no history of abortion or miscarriage. Unfortunately, no documented report is available for his brother.Validation and segregation of the identified variant in all family members were performed by Sanger sequencing using primers flanking the mutation (Forward: 5’-GCTGCTTGATGGGAACCTAC-3’; Reverse 5’-GCTTGTTTTCTCCCAAAAATG-3’)

Drug History:

Antibiotics: Clindamycin, Rifampin, Cefotaxime, Fluconazole, mupirocin ointment, cotrimoxazole, ceftriaxone. IVIG therapy (the patient received IVIG at birth and 21

months old, for unknown reason despite having normal IgG level). Negative allergy history

Laboratory results	Date 1	Date 2	Date 3	Date 4	Date 5	Date 6
	28/1/2009	30/7/2010	25/9/2010	3/10/2010	9/10/2010	31/10/2010
WBC		15080	7300		18490	13120
RBC		3.69 * 10^6				
Hb		8.9	10.9		8.5	8
MCV		73.2				
Plt		799000	457000		1064000	551000
Neut		58/2%	49.2%		73%	79.3%

Lymph		23.9%	39.5%		17%	18%
Mono		11.7%				
NBT		100%				
CRP						
CD2	25					
CD3	66					
CD4	50					
CD8	15					
CD4/CD8	3.3					
CD19	23					
CD16						
CD56						
BMA						No pathologic finding
PBS		PBS: anisocitosis, hypochroic, microcytosis, target cell				No pathologic finding
IgG	IgG:453,	IgG:1358, IgG1:622 IgG2:312 IgG4:128				IgG1:4478 IgG2:1105 IgG3:934 IgG4:195
IgM	45	100				
IgA	5	128				
IgE	5	23				
ESR		74	82			65
CRP		48				>48
CPK						310
Aldolaze						18
C3	105	145				
C4	30	36				
CH50	95	170				
BUN:		9	10			
Cr		0.3	0.3			
PT		12	12.5			
PTT		33 INR=1	39			
Blood Suger		112	115			

Urine analyse		normal	normal			
Urine culture		Candida.	negative			
Stool exam						
Stool culture						
Blood culture		negative				
Calsium		8.5				
Na		133				
K		4.4				
Other		Wright, Coomns Write And 2me Widal =negative , HIV = negative ANA:0.7 negative Anti DS DNA : 12 negative G6pd: normal		Normal production of IL-6, No respounce to TNF-alpha		PHA:2.1 Candida: 1.75

Para-clinical Reports:

Pelvic radiography report
(19 months old) **Pelvic radiography report:** Disseminated osteopenia in bones, Left hip dislocation with no dysplasia
(19 months old) **Pelvic radiography report 2:** Thick Effusion with debris in the left hip with skin fistula. The left hip is dislocated.
(20 months old) **Pelvic radiography report 3:** Both Femurs are in the acetabulum but the left femur's head is deformed

(2 years old) **Pelvic radiography report 4:** There is Fluid effusion in both hips with acetabulum irregularity.The medial side of the Synovial sac in both hips had debris and eco (size:25 mm). There is a collection or pus in the left iliac fossa (20* 13 mm) with calcifications around the lesion, changes in the left hip in favor of osteomyelitis and dislocation.

Elbow radiography report
(19 months old) **Left elbow radiography report:** Inflammation in the deep soft tissue surrounding the elbow joint decreased bone density and periosteal reaction in distal Humerus bone
(19 months old) **Left elbow radiography report 2:** Thick Effusion with debris around the left elbow .
(20 months old) **Left elbow radiography report 3:** Left elbow-joint effusion with echogenic points.
(20 months old) **Left elbow radiography report 4:** Left Elbow had periosteal reactions due to septic arthritis and osteomyelitis, soft tissue inflammation around the elbow joint
(21 months old) **Right elbow sonography :** Hypoeco regions 9*27 mm and 5* 13 mm in lateral arm muscles in ant compartment s in favor of necrosis, abscess, or hematoma, Thick echogenic fluid in the right elbow with dissemination to the anterior capsule of the elbow joint, in favor of puss in the elbow joint.

(20 months old)**Chest and skull x-ray** Disseminated Low bone density ,Osteomyelitis in the left clavicle ,Normal lung and normal skull
(19 months old) **Inguinal ulcer biopsy result:** The microscopic examination demonstrated: congested fibromuscular and adipose tissue, foamy histocytes, and a few giant cell formation. PAS staining is negative for fungal infections. Acid-fast staining was negative for acid-fast bacillus. These finding were in favor of chronic inflammatory process.
(19 months old) **Abdominopelvic sonography:** No pathologic finding, mass, etc. The liver and spleen had normal eco and size. No gallbladder or kidney stone. Kidney, Pancrase, and bladder were normal. Testis had normal size and eco located at the inguinal canal The right hip was normal left hip was dislocated.
(21 months old) **Ecocardiography** Normal cardiac function and anatomy , no vegetation, no PE

Family 5 from Egypt

The proband was a female patient aged 6ms old from Upper Egypt. She was the first offspring of healthy first cousin parents (26 years old father and 24 years old mother). No family history of similar condition was recorded. The pregnancy history was uneventful and she was delivered vaginally with Apgar score 8, 10. Anthropometric measurements at birth were all within normal range; weight was 3 kg (-0.8 SD), length 49 cm (-0.3 SD) and head circumference 33 cm (-0.6 SD). Hypoactivity was noted in the neonatal period and at the age of 2 months the first attack of myoclonic epilepsy appeared. Myoclonic fits were several times per day reached 10-15 times as clusters and were uncontrolled with medications as valproate, levetiracetam and clonazepam. The patient was evaluated at the age of 6 months. No milestones of development were acquired she failed to support the head or reacted to surrounding. Recurrent chest infection was recorded and required hospitalization twice with combinations of antibiotics, antiviral and steroids. Hypoactivity, encephalopathy and failure to thrive were distinguished. The weight was 4.7 kg (-3.25 SD), length 59 cm (-3.4 SD) and head circumference was 37 cm (-3.5 SD). Generally, the girl wasn't reactive and didn't follow objects, she was fairly responded to sounds. She had high forehead, light tangled hair, upturned nose, retruded mandible and low set ears. Cardiac and abdominal examinations were insignificant, however, irregular wheezes and crepitations were present on chest auscultation. Neurologically, there is axial hypotonia, muscle wasting, hypotonia of extremities with some infrequent rigidity and preserved reflexes. Investigations showed normal karyotyping, extended metabolic screening, acylcarnitine profile and organic acid in urine. Blood lactate was mildly elevated (24 mg/dl) and ammonia was within normal range. Echocardiography and ABR were normal while fundus examination showed pale optic disc. Recurrent evaluation of infection profile showed elevation of CRP, microcytic hypochromic anemia and leucocytosis with neutrophilia and sometimes lymphocytosis. Neuroimaging identified mild cortical and central atrophic changes, small vermis and thin corpus callosum.

Family 6 from Syria:

This is a refugee Syrian family in which the parents are unrelated but from the same region in north Syria, with 3 unaffected and 3 affected children. Limited information is available on the first and second kids who died many years ago in Syria:

The first daughter was full term and born normal. She had feeding difficulties, irritability and poor feeding, hospitalised on and off for around 2 weeks, lost weight significantly, cachectic and suddenly died at 4 months of age, less than 2 kg at the time of death.

The second boy was full term and born normal (4 kg at birth), one week in hospital, started losing weight, irritable, encephalopathy and brain atrophy and died at 1.5 months. Proband, full term and born normal, 13 days ICU, poor feeding difficulty, NG feeding, fever first and seizures (at 4 months age), cardiac tumour, spasticity, poor vision and cachectic died 11 months, less than 2 kg at the time of death.

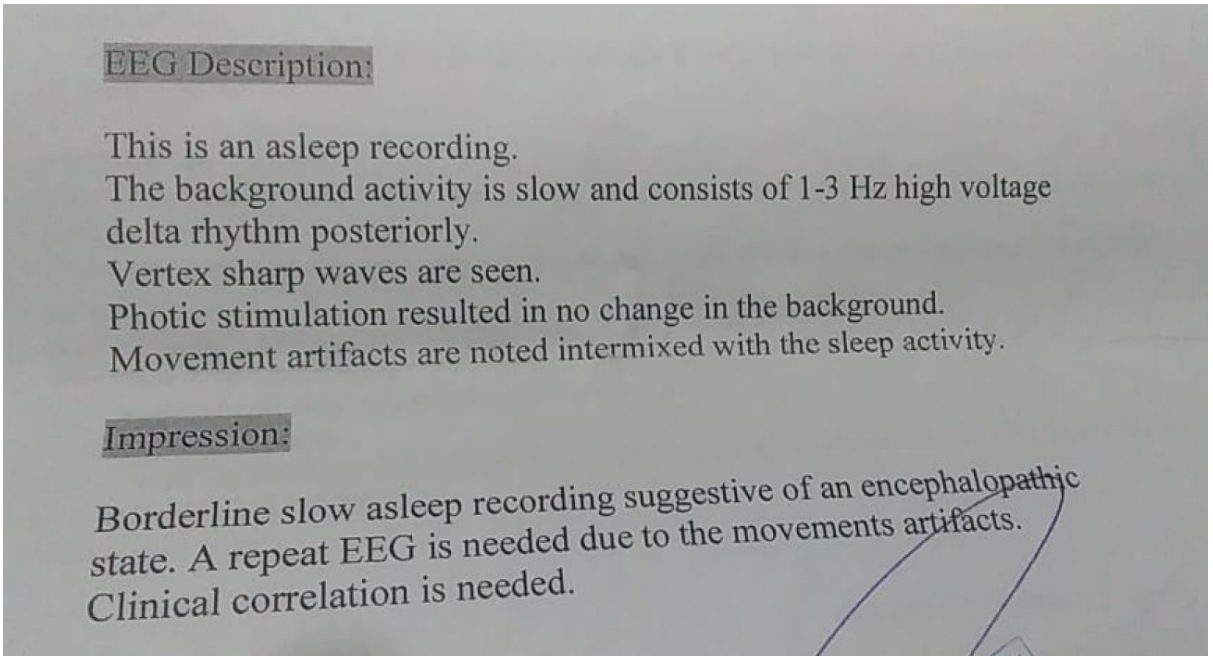

EEG Description:

This is an asleep recording.
The background activity is slow and consists of 1-3 Hz high voltage delta rhythm posteriorly.
Vertex sharp waves are seen.
Photic stimulation resulted in no change in the background.
Movement artifacts are noted intermixed with the sleep activity.

Impression:

Borderline slow asleep recording suggestive of an encephalopathic state. A repeat EEG is needed due to the movements artifacts.
Clinical correlation is needed.

Collection Date	02/12/2019 18:32:08		Report Date	20/12/2019 11:11
Test	**Result**		**Unit**	**Reference**
Order Number	**4020120**			
Test Date	1 03/12/2019 18:31:55			
	Chemistry			
Phosphorous	4.13		mg/dl	2.5 - 4.5
Magnesium	2.16		mg/dl	1.6 - 2.4
	Serology			
CRP	106.4	H	mg/L	<5
Order Number	**4021010**			
Test Date	1 03/12/2019 16:33:17			
	Chemistry			
Ammonia, P	47		ug/dl	27.2 - 102
Order Number	**4021445**			
Test Date	1 04/12/2019 10:38:13			
	Body Fluid			
Protein in CSF	11	L	mg/dl	15 - 45
Specimen type	CSF			
Specimen type	CSF			
Volume	1		ml	
Volume	1		ml	
Appearance	Clear			
Appearance	Clear			
Fibrin Clot	Absent			
Fibrin Clot	Absent			
Viscosity	Normal			
Viscosity	Normal			
Glucose, BF	72		mg/dl	
	Hematology			
CBCD				
WBC	12.2	H	$10^{\wedge}9/L$	4 - 1

Family 7 from Iraq:

The index is a 7-month-old female, born to consanguineous parents from Iraq. Family history is positive. Five older siblings are similarly affected (3 females and 2 males). Four of them died during early infancy (surviving up to 3 years), the living affected female sibling is in critical condition. The index patient presented feeding difficulties soon after birth. She has neurodevelopmental delay, failure to thrive and brain atrophy. Her older affected sister is currently 4-year-old, she has feeding difficulties, neurodevelopmental delay, joint contractures, and brain atrophy.

An expanded new-born screening performed at 23-days-old had normal results. No evidence of Hypothyroidism, Galactosemia, Cystic Fibrosis, Congenital Adrenal Hyperplasia, GGPD and Biotinidase Deficiency. There is no indication of amino acid disorders such as: Hyperphenylalaninemia (PKU), Maple Syrup Urine Disease (MSUD), Tyrosinemia type-I, II and 111, Argininosuccinic Aciduria, Citrullinemia, Homocystinuria, Argininemia and Non-Ketotic Hyperglycinemia.

In addition, the acylcarnitines do not show any indication of metabolic diseases. There is no evidence of the following organic acid disorders: 3-Hydroxy-3-Methylglutaric Aciduria (HMG), Glutaric Acidemia (GA) Type I and II, Isovaleric Acidemia (IVA), 3-Methylcrotonyl-CoA Carboxylase Deficiency (3-MCC), Methylmalonic Acidemia (MUT), Malonic Aciduria, B-Ketothiolase Deficiency (BKT), Propionic Acidemia (PROP), and Multiple Carboxylase Deficiency (MCD). And also, no evidence of the following fatty accid oxidation disorders: Carnitine Uptake Defect (CUD), Long Chain L-3 hydroxyl-CoA Dehydrogenase Deficiency (LCHAD), Median Chain Acyl-CoA Dehydrogenase Deficiency (MCAD), Trifunctional Protein Deficiency (TFP), Very Long Chain Acyl-CoA Dehydrogenase Deficiency (VLCAD), and Carnitine Palmitoyltransferase (CPT) I and II.

No evidence of adenosine deaminase severe combined immunodeficiency (ADA-SCIO), which is caused by a deficiency of the enzyme ADA and is the second most common SCIO. There is no evidence, also, of X-Linked Adrenoleukodystrophy (X-ALD).

Additionally, thorax X-ray was normal, Brain CT showed brain atrophy, EEG was abnormal (focal discharges), auditory evoked potentials (4-month-old) showed normal hearing but immature brain stem waves, with recommendation to follow up.

Informed consents were provided, including consent for scientific publication. The form contains a section for consent for genetic testing related to the disease(s) of the individual, and consent for research (related to the main concern, but implicating genes not yet associated with human diseases). The informed consent form is available upon request with Centogene. Exome and genome sequencing were performed as previously described [18,19]. Validation and segregation of the identified variant in all family members were performed by Sanger sequencing using primers flanking the mutation (Forward: 5'-GCTGCTTGATGGGAACCTAC-3'; Reverse 5'-GCTTGTTTTCTCCCAAAAATG-3')

Family 8 from Turkey:

The male proband (II:3) is the third born child of healthy consanguineous Turkish parents, born at 38 weeks of gestation following an uncomplicated pregnancy and vaginal delivery. He had two healthy sisters and family history was unremarkable. Anthropometric measurements at birth were within normal limits [Birth weight: 3100g (50-75p, -0.74 SD), Birth length: 49cm (50-75p, -0.44 SD), Head circumference: 35cm (75-90p, -0.4 SD)]. Soon after birth he developed signs of respiratory distress, which required intervention by ventilatory support in the intensive care unit (ICU). Due to paracardiac infiltrates in the chest X-ray, he was treated with broad-spectrum antibiotics. He received phototherapy for neonatal jaundice and anti-E minor blood group incompatibility was detected.

Complete blood count (CBC) revealed neonatal anemia (hemoglobin: 10 g/dl) with MCV of 111fl and reticulocyte ratio of 4.48%. Absolute neutrophil count and absolute lymphocyte counts were normal for age and he never became lymphopenic or neutropenic throughout his life. LDH dramatically was elevated (3217 U/l) and peripheral blood smear showed presence of normoblasts, spherocytes and schistocytes. In order to identify the underlying cause of congenital anemia, bone marrow aspiration was performed which showed intermediate cellularity, micromegakaryocytes, and erythroid hypoplasia with unremarkable changes in myeloid lineage. Hemoglobin electrophoresis and osmotic fragility tests were normal. He required regular transfusions throughout his life due to persistent anemia.

Throughout his life, the proband was hypotonic with fair hair and skin, but had no apparent dysmorphic or skeletal abnormalities. Laboratory work-up revealed significantly elevated liver enzymes (ALT: 248U/l, AST: 1291U/l) and hyperbilirubinemia (total bilirubin: 17.25mg/dl, direct bilirubin 1.07mg/dl) and was treated by ursodeoxycholic acid. He was given amlodipine as a result of continuous high blood pressure. He had poor feeding, persistent vomiting and mild respiratory distress. Size of liver and spleen were normal by abdominal ultrasonography in the first month of life. Renal artery and vein doppler ultrasound was normal and the echocardiogram showed atrial septal defect (ostium secundum), which was not apparent on follow-up. During the course, he continued to have repeated pulmonary infections, accompanied by elevation in C-reactive protein (CRP) levels and received broad-spectrum antibiotics. Under antibiotic treatment CRP levels decreased but anemia was persistent (Hb: 8.3g/dl at 2 months). Unexpectedly, he developed swollen left knee with inflammatory signs at 6 months, which lasted about 2 weeks and accompanied by mild thickening of synovial wall and increased bursal fluid on ultrasound. Due to his fair hair and skin accompanied by recurrent pulmonary infections, primary immune deficiency syndromes with pigmentation abnormalities, such as Chediak-Higashi syndrome or Griscelli syndrome were considered, but normal immunological assays and microscopic examination of proband's hair ruled out these diagnoses.

Starting from his second month of life, he developed drug-resistant focal epilepsy; received multiple antiepileptic medications, including clobazam, topiramate, carbamazepine, levetiracetam and pyridoxine, but without any improvement. EEG at

2 months revealed asynchronous multifocal epileptiform discharges initially, and left temporal dysfunction with focal epileptic discharges. at 6 months. Metabolic screening tests, including tandem mass spectroscopy and urinary organic acids, were normal. As the proband's multisystemic findings were highly suggestive of a metabolic/mitochondrial disorder, muscle biopsy was performed at the age of 5 months, which showed subtle mitochondrial proliferation, mild cytochrome-C-oxidase deficiency and presence of partially diastase-resistant Periodic Acid-Schiff (PAS) stained granules. These findings were suggestive for mitochondrial dysfunction and glycogen storage disease. Brain MRI at seven-months showed dilatation of all ventricles, cortical thinning and a decrease in cerebral white matter discordant with age. The concurrent MR spectroscopy was normal.

He was admitted to the hospital several times throughout his life mainly for transfusion dependent anemia, recurrent pulmonary infections and intractable seizures. He was hypotonic, microcephalic and undernourished with weight, length and head circumference below 3rd percentile after 6 months. He never gained any developmental milestones and passed away at the age of 1 due to respiratory failure.

After the male proband's death, his sister (II:4), the fourth child of the family, was born at 38th gestational week via uncomplicated vaginal delivery. Prenatal history was not remarkable. She also developed neonatal jaundice and received phototherapy. Her hemoglobin at birth was low (9 g/dl) like her affected brother. CBC was repeated at 2 months due to remarkable pallor and fatigue, which revealed marked anemia with a hemoglobin of 7.8 g/dl and high reticulocyte ratio of 3.19%. Her blood smear revealed polychromasia, hypochromia, anisocytosis and basophilic stippling. After receiving folic acid treatment her hemoglobin levels returned to normal and symptoms improved. Imaging studies included an abdominal ultrasonography showing mild renal pelvis dilation. Abdominal ultrasonography showed mild renal pelvis dilation. She did not have fair hair unlike her brother. Her anemia was under control with no additional symptoms and she did not require blood transfusions. Currently she is 13 months old and has reached developmental milestones timely and did not develop epilepsy.

The marked discordance of phenotypic expression between the 2 affected siblings prompted us to look for a blended phenotype in the proband caused by at least 2 independently segregating Mendelian phenotypes. We performed whole exome sequencing (WES) in the proband and due to apparent autosomal recessive inheritance, we focused on homozygosity (see the figure below). Twelve >4 Mbp runs of homozygosity (uninterrupted blue stretches in the middle portion of figure) were identified in the WES data using HomSI [1]. In these regions, 12 candidate variants were present. One of these variants explained the congenital anemia phenotype in both siblings through a novel homozygous missense mutation in *CDIN1* (aka. *C15orf41*) (c.58C>A, p.Pro20Thr), a newly described gene leading to congenital dyserythropoietic anemia type 1 [MIM 615631]. The proband also had a hypofunctional homozygous c.1441G>A (p.Ala481Thr) variation in *OCA2* on chromosome 15, responsible for regulating skin, hair and iris pigmentation [2]. This variant was absent in the sister, indicating that it is associated with the fair hair in the

proband, which is uncommon in his family. Based on the presence of two rare homozygous variants within the same ~60 Mbp homozygous stretch on chromosome 15, the possibility of uniparental disomy or large deletion was explored. MLPA which covers the critical region for Prader-Willi Syndrome within this genomic stretch on chromosome 15 ruled out both possibilities. The most probable candidate for explaining the divergent neurological findings found in the proband was the only highly damaging nonsense mutation that segregated in the family—a novel nonsense mutation in C2orf69 (c.929G>A, p.Trp310Ter) [MIM 619219]. The clinical and genetic findings for family 8 have also been presented in ESHG 2020 [3].

Informed consent forms for genome-wide high-throughput sequencing were obtained from each individual, which was in accordance with the ethical standards of the Declaration of Helsinki. The DNA from family members was archived in the inherited bone marrow failure syndrome registry and Genome-wide studies were performed in Hacettepe University Medical Genetics Exome Facility. Briefly, DNA libraries from peripheral blood leukocytes for WES were prepared by Ion AmpliSeq Exome RDY kit (ThermoFisher Scientific) and subsequently sequenced by Ion Proton semiconductor sequencer (ThermoFisher Scientific). IonReporter software was used for alignment, variant calling and annotation. Rare and likely damaging variants in homozygosity regions were verified and available family members were genotyped by Sanger sequencing.

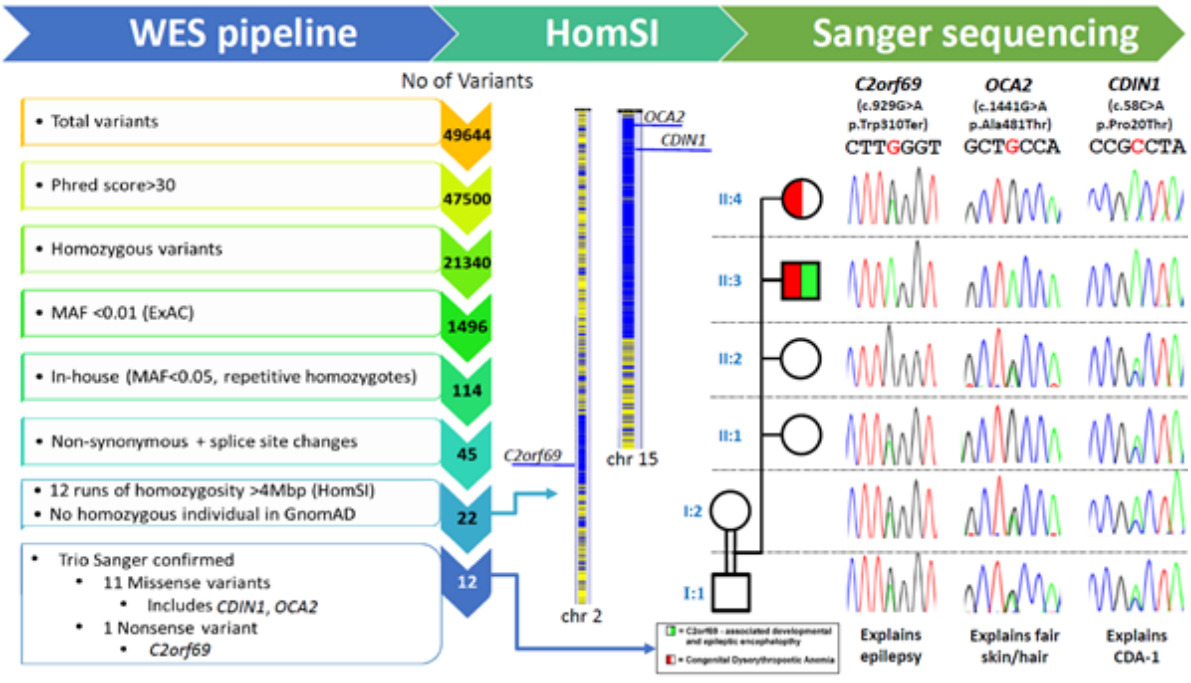

Supplemental Figures

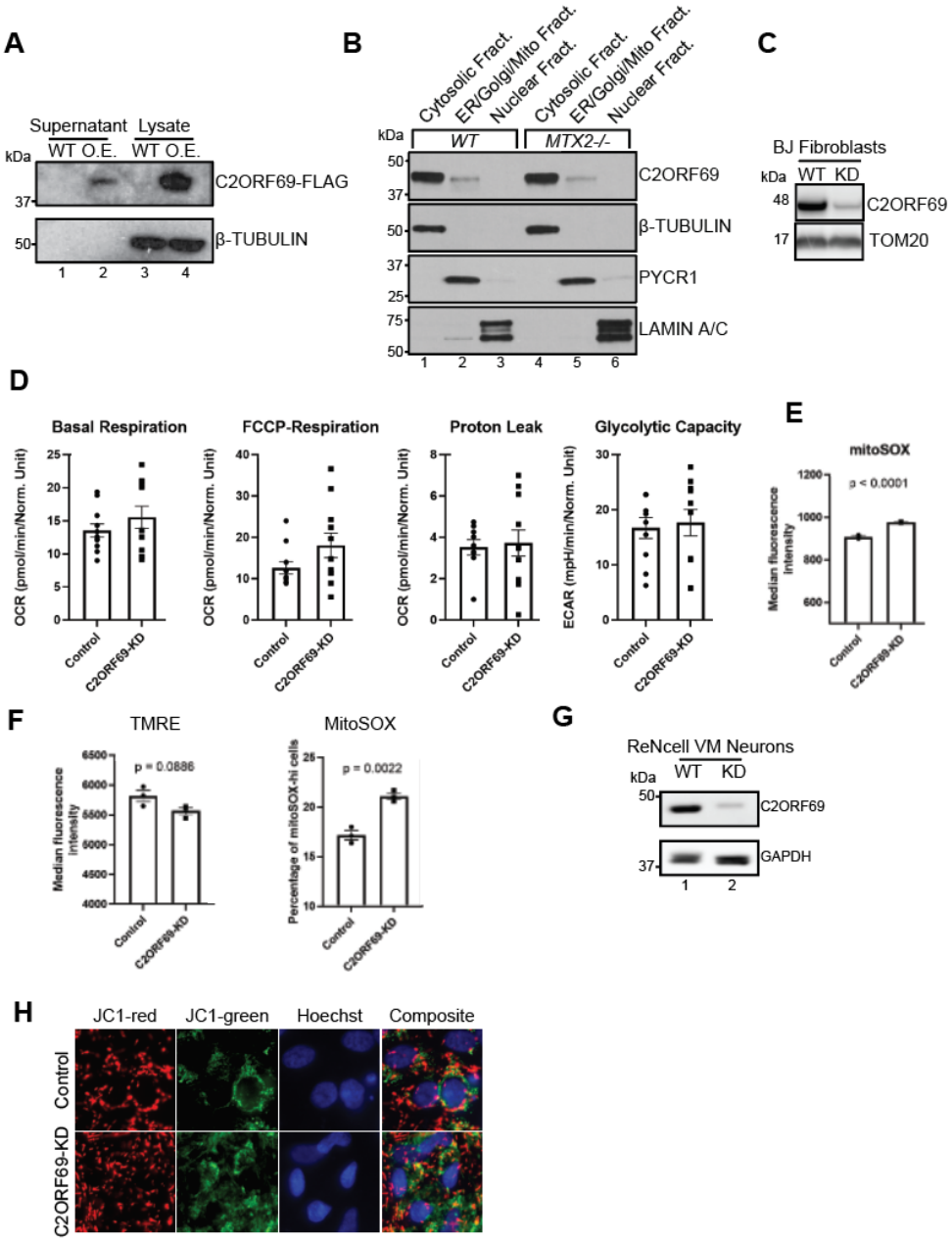

Figure S1: C2ORF69 knockdown efficiency in human cultured cells

(A) Overexpressed Flag-tagged C2orf69 can be found in the supernatant of BJ-TERT cells. The majority is seen in the cell lysate.

(B) Endogenous C2orf69 is mainly found in the cytoplasmic fraction of wt and MTX2 knockout human fibroblasts. A smaller fraction is seen with the mitochondrial extract.

(C) siRNA-mediated knockdown efficiency of endogenous C2orf69 measured by western blotting on BJ Fibroblasts.

(D) Agilent Seahorse mito-stress (3 left panels) and GlycoStress (rightmost panel) test on control and C2orf69 knockdown (KD) fibroblasts.

(E) Mitochondrial ROS sensitive dye MitoSOX (5 uM) measurement of mito-ROS production in control and C2orf69 knockdown (KD) fibroblasts. Each dot represents one well of cultured cells. Data are mean +/- SEM, p-value = unpaired student's t-test.

(F) Mitochondrial membrane potential in control and C2orf69 knockdown (KD) fibroblast measured by TMRE dye (100 nM) by flow cytometry. The same samples were stained with mitochondrial ROS sensitive dye MitoSOX (5 μM). Each dot represents values derived from one well of cells. Data are mean +/- SEM, p-value is derived from unpaired t-test.

(G) siRNA-mediated knockdown efficiency of endogenous C2orf69 measured by western blotting on ReNcell VM Neurons.

(H) Representative images of ReNcell VM neurons stained with ratiometric JC-1 dye.

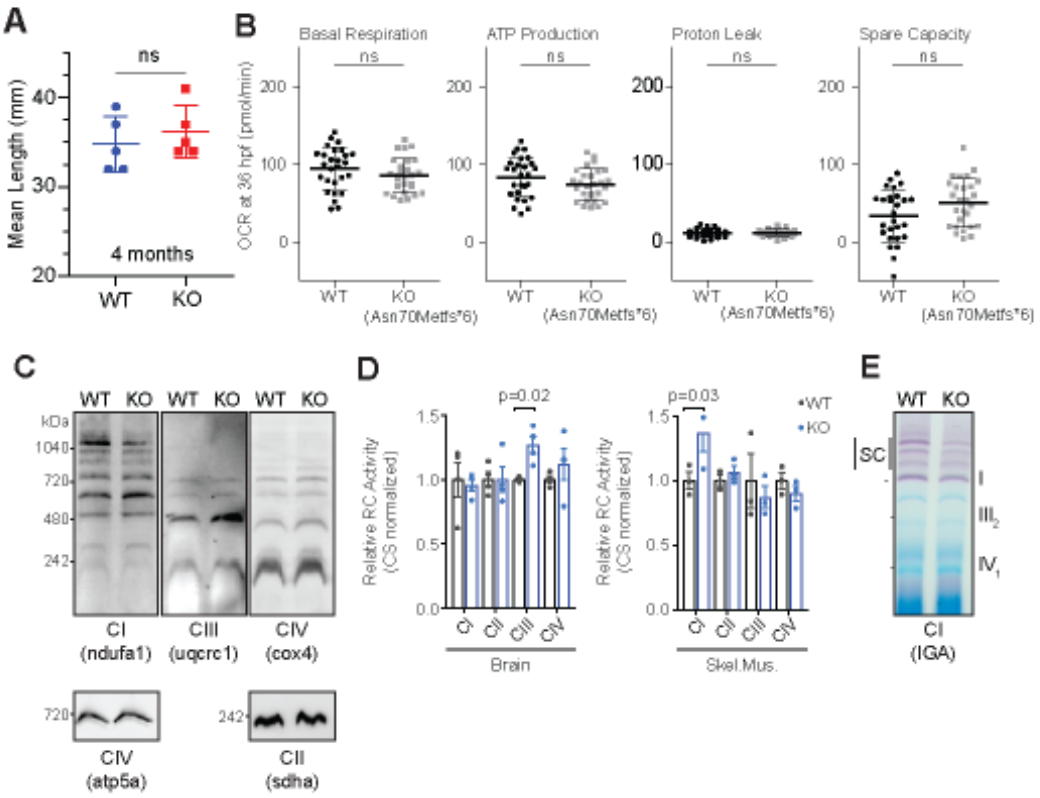

Figure S2
HH. Wong *et al.*, (2021)

Figure S2: C2ORF69 knockout fish have mild respiration defects.

(A) C2orf69 knockout fish are born at Mendelian ratios and at 4 months of age have the same length as their wiltdype siblings.

(B) C2orf69 knockout embryos at 36 hpf show no oxidative respiration defects as measured by a Seahorse mito-stress assay.

(C) Blue native PAGE of purified skeletal mitochondria and western blot for ETC complexes I-IV with the indicated proteins. SC=supercomplexes. Results are representative of 3 independent experiments.

(D) Respiratory chain enzymatic assays of CI - CIV of WT and KO skeletal muscle (left) and brain (right) homogenates. Data are represented as mean +/- SEM, p = p-value from unpaired student's t-test. n=4 biological replicates. Each dot is an average of 3 technical replicates of each biological replicate. Data are mean +/- SEM, p value = unpaired student's t-test.

(E) In-gel assay for CI activity following clear native PAGE of purified skeletal mitochondria. Results are representative of 2 independent experiments.

		Family 1		Family 2	Family 3			Family 4		Family 5	Family 6	Family 7	Family 8
	HPO	Case 1	Case 2	Case 3	Case 4	Case 5	Case 6	Case 7	Case 8	Case 9	Case 10	Case 11	Case 12
Origin		Turkey	Turkey	Tunisia	Saudi Arabia			Iran		Egypt	Syria	Iraq	Turkey
Sex		Male	Male	Female	Male	Male	Female	Male	Male	Female	Male	Female	Male
Recessive inheritance	HP:0000007	+	+	+	+	+	+	+	+	+	+	+	+
Gene (MIM619219)		*C2orf69*		*C2orf69*	*C2orf69*			*C2orf69*		*c2orf69*	*C2orf69*	*C2orf69*	*C2orf69*
C2orf69 variant (NM_153689.5)		c.298delC		c.280delG	c.588_592delTTTAA			c.298delC		c.311_313del	c.909_925del	c.298delC	c.929G>A
Predicted protein change (Q8N8R5)		p.(Q100Sfs*18)		p.(E94Sfs*24)	p.(N196Kfs*4)			p.(Q100Sfs*18)		p.(L104_Y105delinsH)	p.(S304Lfs*29)	p.(Q100Sfs*18)	p.(W310*)
Observed protein change (Q8N8R5)		p.0		n.t.	n.t.			p.0		n.t.	n.t.	p.0	n.t.
Clinical synopsis													
Disease onset		3 months	3 months	Congenital	n.a.	n.a.	Congenital	3 months	4 months	2 months	4 months	neonatal	neonatal
Antenatal findings/pregnancy		normal, 41 week ,	normal, 36 weeks,	normal, 41 week , NVD	n.a.	n.a.	preterm, needed	41 weeks, CS	41 weeks, CS	41 week, NVD	41 weeks, CS	n.a.	38 weeks, NVD
Head Circumference at birth (cm)		normal	n.a.	35	n.a.	n.a.	n.a.	normal	normal	33 (-0.6 SD)	normal	n.a.	35 (-0.4 SD)
Birth Weight (kg)		3.75	2.3	3.1	n.a.	n.a.	2.12	3.5	3.7	3.0 (-0.8 SD)	3.5	3.5	3.1 (-0.74 SD)
Birth Length (cm)		normal	45	50	n.a.	n.a.	n.a.	52	50	49 (-0.3 SD)	normal	n.a.	49 (-0.44 SD)
Age at last exam		12 months	6 months	18 months	n.a.	n.a.	6 months	24 months	n.a.	6 months	6 months	6 months	7 months
Head circumference (cm)		39 (-5 SD)	39 (-3.1 SD)	39.5 (-6 SD)	n.a.	n.a.	36 (-6 SD)	n.a.	n.a.	37 (-3.5 SD)	n.a.	n.a.	37 (-5.5 SD)
Failure to thrive, (weight at last exam, kg)	HP:0001508	+, (4.9, -5.3 SD)	+, (4.3, -4.3 SD)	+, (6.5, -3 SD)	n.a.	n.a.	+, (4.6)	+	n.a.	+, 4.7 (-3.25 SD)	+, 2.5 (-5 SD)	+	5.8 (-3 SD)
Post-natal short stature, (length at last exam, cm)	HP:0004322	+, (68, -2.7 SD)	+, (58, -3.7 SD)	+, (85)	n.a.	n.a.	+, (53)	n.a.	n.a.	+, 59 (-3.4 SD)	n.a.	+	60 (-3.5 SD)
Deceased, (age of death)		+, (18 months)	alive (in critical	+, (32 months)	+, (n.a.)	+, (18 months)	+, (24 months)	+, (29 months)	+, (11 months)	+, (9 months)	+, (9 months)	alive (in critical	+, (12 months)
Cause of death		pneumonia	-	status epilepticus	n.a.	n.a.	n.a.	pneumonia	pneumonia	pneumonia	cardiac arrest	n.a.	pneumonia
Brain anomalies													
Developmental delay	HP:0001263	+	+	+	+	+	+	+	+	+	+	+	+
Secondary microcephaly	HP:0005484	+	+	+	+	+	+	n.a.	n.a.	+	-	+	+
Cerebellar atrophy/Dandy Walker variant	HP:0001272	+	+	-	n.t.	+	+	-	-	+	-	+	-
Dysgenesis of corpus callosum	HP:0006989	+	+	-	n.a.	n.a.	n.a.	+	+	+	+	+	-
CNS hypomyelination	HP:0003429	+	+	-	n.a.	n.a.	n.a.	n.a.	n.a.	+	+	+	+
Cerebral atrophy	HP:0002059	+	+	+	n.a.	n.a.	n.a.	n.a.	n.a.	+	+	+	+
Basilar impression	HP:0005758	+	+	-	n.a.	n.a.	n.a.	n.a.	n.a.	+	-	n.a.	-
Cerebellar vermis atrophy	HP:0002335	+	+	-	n.a.	n.a.	n.a.			+	-	-	-
Cerebral cortical atrophy	HP:0006855	+	+	-	n.a.	n.a.	n.a.	n.a.	n.a.	+	+	+	+
Seizures	HP:0001250	+	+	+ (focal, pharmacoresistant)	+ (intractable)	+	+ (focal)	+ (absent seizures, several episodes)	n.a.	+ (Myoclonic, several times a day)	+ (tonic)	+ (Focal and Myoclonic)	+ (intractable, focal)
Severely reduced visual acuity	HP:0001141	+	+	+, (abnormal pursuit)	n.a.	n.a.	n.a.	-	-	+	+	+	n.a.
Optic nerve hypoplasia	HP:0000609	+	+	-	n.t.	+	n.t.	-	-	n.t.	n.t.	n.t.	-
Immune anomalies													
Recurrent fever	HP:0001954	+	+	+	n.a.	n.a.	n.a.	+	+	+	-	+	+
Inflammatory arthritis	HP:0001369	-	-	-	n.a.	n.a.	n.a.	+	+	-	-	-	+ (knee, once)
Septic arthritis	HP:0003095	-	-	-	n.a.	n.a.	n.a.	+	+	-	-	-	-
Aseptic osteomyelitis	HP:0002754	+ (tibia, elbow, hip)	-	-	n.a.	n.a.	n.a.	+ (elbows, hip, clavicle)	n.a.	-	-		-
Elevated C-reactive protein level	HP:0011227	+	+	-	n.a.	n.a.	n.a.	+	n.a.	+	-	-	+
Pneumonia	HP:0002090	+	+	+	n.a.	n.a.	n.a.	+	+	+	+		+
Hypochromic microcytic anemia	HP:0004840	+	+	n.t.	n.a.	n.a.	n.a.	+	n.t.	+	n.a.	n.a.	Anemia due to Congenital Dyserythropoietic Anemia
Response to steroids		n.t.	n.t.	n.t.	n.t.	n.t.	n.t.	n.t.	n.t.	+	n.a.	n.a.	n.t.
Other phenotypes													
Muscular hypotonia	HP:0001252	+	+	+	n.a.	+	+	-	-	+	+	+	+
General muscle wasting	HP:0009055	+	+	+	n.a.	n.a.	n.a.	+	n.a.	+	+	+	+
Abdominal distention	HP:0003270	+	+	-	n.a.	n.a.	n.a.	+	+	n.a.	-	-	-
Muscular spasticity	HP:0001257	-	-	+	n.a.	n.a.	n.a.	+	+	n.a.	+	n.a.	-
Hepatomegaly	HP:0002240	+	+	-	n.a.	n.a.	n.a.	-	-	-	-	n.a.	-
Osteopenia	HP:0000938	+	n.t.	-	n.a.	n.a.	n.a.	+	+	n.a.	n.a.	n.a.	n.t.
Brittle hair	HP:0002299	+	+	-	n.a.	n.a.	+	-	-	+	+ (sparce)	-	-
Fair hair	HP:0002286	+	+	-	n.a.	n.a.	+	-	-	+	-	-	+
Dry hair	HP:0011359	+	+	-	n.a.	n.a.	+	-	-	+	-	-	-
	-: negative	+: affirmative	n.t.: not tested	n.a.: not available	CS: Caesarean	NVD: Normal							

Unabridged Supplemental Table1

Supplemental Methods

List of antibodies used

Primary antibodies used were anti-C2orf69 (rabbit, 1:500 in 5% milk in TBST, Abcam #188870), anti-Laminin A/C (rabbit, 1:1000 in 5% BSA in TBST, Cell Signalling #2032), anti-PYCR1 (rabbit, 1:2000 in 5% milk in TBST, Proteintech #13108-1-AP), anti-β-Tubulin (mouse, 1:500 in 5% milk in TBST, Merck #MAB3408), anti-MTCOI, 1:3000 (Abcam, ab14705), anti-TOMM20, 1:500 (Proteintech, 11802-1-AP), anti-TIM23, 1:5000 (Proteintech, 11123-1-AP) and anti-CS, 1:2000 (Santa Cruz, SC-390693).

List of primers used

Two guide RNAs against exon 1 of *c2orf69* was used with the following targeting sequences, 5'-AGAGCAGAACATCATTGACG-3'; 5'-GGAAAATGACCGCTGCAACG-3'.

Quantitative real time PCR

Primers used to determine gene expression in zebrafish:

Gene	Forward	Reverse
TNFα	GCTGGATCTTCAAAGTCGGGTG TA	TGAGTCTCAGCACACTTCCATC
TGFβ	CCTTGCTTGCTGGACAGTTT	AATCCGCTTCTTCCTCACCA
TGFβ1a	CCTGCACCTACATCTGGAATG	TGAGAAATCGAGCCATGAACC

TGFβ1b	ACAATGAAGGAGAAGCAGGAG	TTCTAACACAGCAACCCTCAG
IL1β	GGACTTCGCAGCACAAAATGAA	TTCACTTCACGCTCTTGGATGA
Scn1a	GAGCGGTTTGACCCCAATG	GGCAATGCGTAATGGAGGAT
Scn8aa	TGGCTGGATTTCATGGTCATC	GAATGTGCGCAGAGCTGACA
Scn8ab	GCCGTGGCTCTCTCTTCGT	AGCCAGCGGGTTAATTCGA
β-actin	AGAAAATCTGGCACCACACC	AGAGGCGTACAGGGATAGCA

Seahorse analysis on zebrafish larvae

Zebrafish Seahorse XFe24 Mito Stress experiments were performed with minor amendments to Stackeley et al. 2011[1]. Ten single dechorionated 26hpf embryos per line were trapped under meshes in a 24 well islet capture plate. Embryos were sequentially exposed to 9.4 µM Oligomycin A (Sigma 75351), 2.5 µM FCCP (Sigma C2920) and finally 2 µM of both Rotenone and Antimycin A (Sigma R8875/A8674). For basal respiration 8 measurements were taken (Mix: 2 min, Wait: 1min, Measure: 2 min), followed by 16, 8 and 20 for the drug-modified respiration stages. Three replicate runs were performed. Calculations were performed according to manufacturer's instruction.

Constructs and site directed mutagenesis

The wild type C-terminus Flag-tagged C2orf69 (C2orf69-Flag) ORF construct (was purchased from Genscript (#OHu26166). To obtain ORF encoding for patient's LY104_Y105delinH, deletions of 3 nucleotides from the wild type C2orf69 was introduced by PCR, using the Q5 Site-Directed Mutagenesis kit (New Englands Biolabs) with the following primers: Fwd: ATTTCCCTGGGGATGTGCAG and Rvs: GGACGTGATGCTGGGGCG. PCRs were run for 24 cycles of 10 s at 98°C, 30 s at 57°C and 30 s at 72°C. The resulting mutant plasmids were verified by DNA sequencing. The Flag-tagged C2orf69 construct depleted of the first 24 amino acid encoding for the MTS (Δ-MTS-C2orf69-Flag) were generated with Genscript via gene synthesis.

Blue and Clear Native PAGE

Mitochondria were further isolated by centrifuging the homogenates described above at 600 × *g* for 5 min to clear intact myofibrils and heavy cell debris and then spun at 7000 × *g* for 15 min to isolate the desired mitochondrial fraction. 50 µg of purified mitochondria were extracted with 8 g/g digitonin and resolved on 3-12% Native PAGE gels (Thermo Fisher) for Western blotting (blue native) or Complex I in-gel assay (clear native) according to [2].

Statistical analysis

Continuous variables are presented as means with standard deviations. Comparisons were performed with parametric tests for normally distributed data or nonparametric tests when not satisfying this criterion. For multiple comparisons, adjusted P values and confidence intervals were calculated with Šídák correction in one-way ANOVA tests or Bonferroni correction in Fisher's Exact tests. Detailed statistical methods used for individual assays are described in the figure legends.

Supplemental References

1. Görmez, Z., Bakir-Gungor, B., Sagiroglu, M.S. (2014). HomSI: a homozygous stretch identifier from next-generation sequencing data. Bioinformatics. 30, 445-447.

2. Yuasa, I., Umetsu, K., Harihara, S., Miyoshi, A., Saitou, N., Park, K.S., Dashnyam, B., Jin, F., Lucotte, G., Chattopadhyay, P.K., Henke, L., Henke, J. (2007). OCA2 481Thr, a hypofunctional allele in pigmentation, is characteristic of northeastern Asian populations. J. Hum. Genet. 52, 690-693.

3. Gurel, A., Unal, S., Yarali, N., Simsek Kiper, P., Ceylaner, S., Bilir, O.A., Gumruk, F., Akarsu, N.A., Cetinkaya, A. High intrafamilial variability in a C15orf41 associated Congenital Dyserythropoietic Anemia family indicates involvement of C2orf69 in infantile epilepsy. Eur J Hum Genet, 2020; 28 (Suppl 1): 302 (Abstract no P07.08.A) https://doi.org/10.1038/s41431-020-00739-z

4. Stackley, K.D., Beeson, C.C., Rahn, J.J., and Chan, S.S.L. (2011). Bioenergetic profiling of zebrafish embryonic development. PLoS One *6*, e25652.

5. Jha, P., Wang, X., and Auwerx, J. (2016). Analysis of Mitochondrial Respiratory Chain Supercomplexes Using Blue Native Polyacrylamide Gel Electrophoresis (BN-PAGE). Curr. Protoc. Mouse Biol. *6*, 1–14.